ACS OMEGA

http://pubs.acs.org/journal/acsodf

Article

# Origin and Geochemical Implications of Hopanoids in Saline Lacustrine Crude Oils from Huanghekou East Sag and Laizhouwan Northeastern Sag, Bohai Bay Basin

Congkai Niu, Dujie Hou,* Xiong Cheng, Xu Han, Yan Li, and Yaxi Li

Cite This: *ACS Omega* 2021, 6, 30298−30314

Read Online

ACCESS | Metrics & More | Article Recommendations | Supporting Information

**ABSTRACT:** A suite of low-mature crude oils (five high-sulfur oils and six low-sulfur oils) from the Huanghekou and the Laizhouwan Sags, Bohai Bay Basin, are analyzed to investigate the fate of the hopanoids. Abundant hopanes, such as secohopanes, 25-norhopanes, benzohopanes, aromatized secohopanes, and sulfide hopanes, are identified, and their carbon isotope compositions are determined. Varying $^{13}C$ isotope values of $C_{31}$ hopane (−38.7−34.0‰) and $C_{29\text{-}30}$ hopanes (−38.5−31.5‰) suggest different bacterial sources of these compounds. The presence of 25-norhopanes with enriched heavy carbon isotopes in severely biodegraded oils suggests that they are microbially mediated products. The detection of the isotopically depleted $C_{29}$ and $C_{30}$ D-ring-8,14-secohopanes (−45.6−41.2‰) indicates that secohopanes are from methane-oxidizing bacteria (methanotrophs). The presence of isorenieratane, lower aryl isoprenoid ratios, and a good correlation between the sulfur content and the gammacerane index indicate the presence of green sulfur bacteria (Chlorobiaceae) under photic zone euxinic conditions. Water column stratification results in good preservation of the organic matter, and it is in favor of diversity of aquatic microorganisms. The ratios of $C_{35}/C_{34}$ sulfide hopane, $C_{35}$ sulfide hopane-2/$C_{35}$ sulfide hopane-1, and $C_{35}/C_{34}$ benzohopane are influenced by the reducing environments in this region. In addition, the D-ring monoaromatized 8,14-secohopanoid/(D-ring monoaromatized 8,14-secohopanoid + benzohopanes) and $C_{31}-C_{35}$ secomoretanes/secohopanes are affected by the maturity. We hypothesize that the reducing environments and thermal effects are important markers for the hopanoid transformation, including the incorporation of inorganic sulfur in substituting functional groups, cyclizing, aromatizing, and opening ring C of the hopanoids.

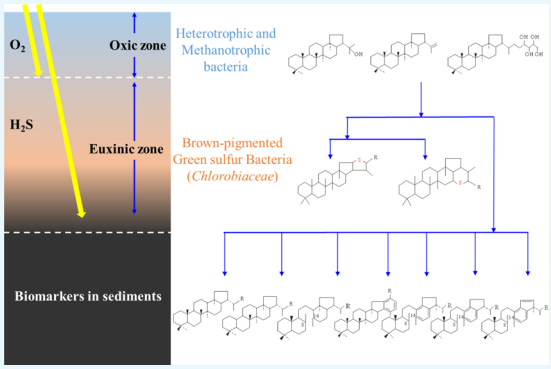


## 1. INTRODUCTION

Hopanoids are ubiquitous in sediments and crude oils and are an important indicator for bacteria.[1−3] Previous research studies have shown that hopanoids are more resistant to biodegradation,[4−7] natural weathering processes,[8,9] and thermal effects[10,11] than *n*-alkanes, isoprenoids, and bicyclic sequiterpanes. In addition, the spatial configuration of hopanoids regularly evolutes from the initial biological isomers to the following geological counterparts.[12] Therefore, many parameters of hopanoids are used to reflect the depositional environment,[13] thermal maturity,[14] and degree of biodegradation.[15] Hopanoids have been used as molecular markers for oil−oil and oil−source rock correlation in petroleum geochemistry. A major source of hopanoids > $C_{30}$ in sediments is formed from the cleavage of the extended side chain of $C_{31}-C_{35}$ bacteriohopanepolyols in some cyanobacteria and heterotrophic and methanotrophic bacteria.[16−18] The number, position, and nature of functional groups in the extended side chain might represent different species of bacteria.[19−22] For example, hopanoids with five functional groups at the side chain and an additional hydroxyl group at the $C_{30}$ or $C_{31}$ position were found in cyanobacteria[20] and methanotrophic bacteria (with an amino group at $C_{35}$[22]). Hopanoids < $C_{30}$ are mainly formed from diplopterol and diploptene without a long side chain at C-22, which can be found in almost all hopanoid-producing bacteria.[23] Because of the comprehensive impact of the origin, depositional environment, and diagenetic effects, the hopanoids occur in many novel types with various structures, such as hopenes,[24,25] isohopanes,[26,27] rearranged hopanes,[28−32] aromatized hopanes,[33,34] sulfur-containing hopanes,[34−40] and nitrogen-containing hopanes.[41,42] Intriguingly, most hopanoid precursors were found in aerobic bacteria,[23] although their biosynthesis does not require oxygen. However, some hopanoids were also found in anaerobic bacteria, such as *planctomycetes*,[43] *Petrosia* sp.,[44] *Desulfovibrio*,[45]

**Received:** May 26, 2021
**Accepted:** October 22, 2021
**Published:** November 4, 2021





https://doi.org/10.1021/acsomega.1c02762
*ACS Omega* 2021, 6, 30298−30314

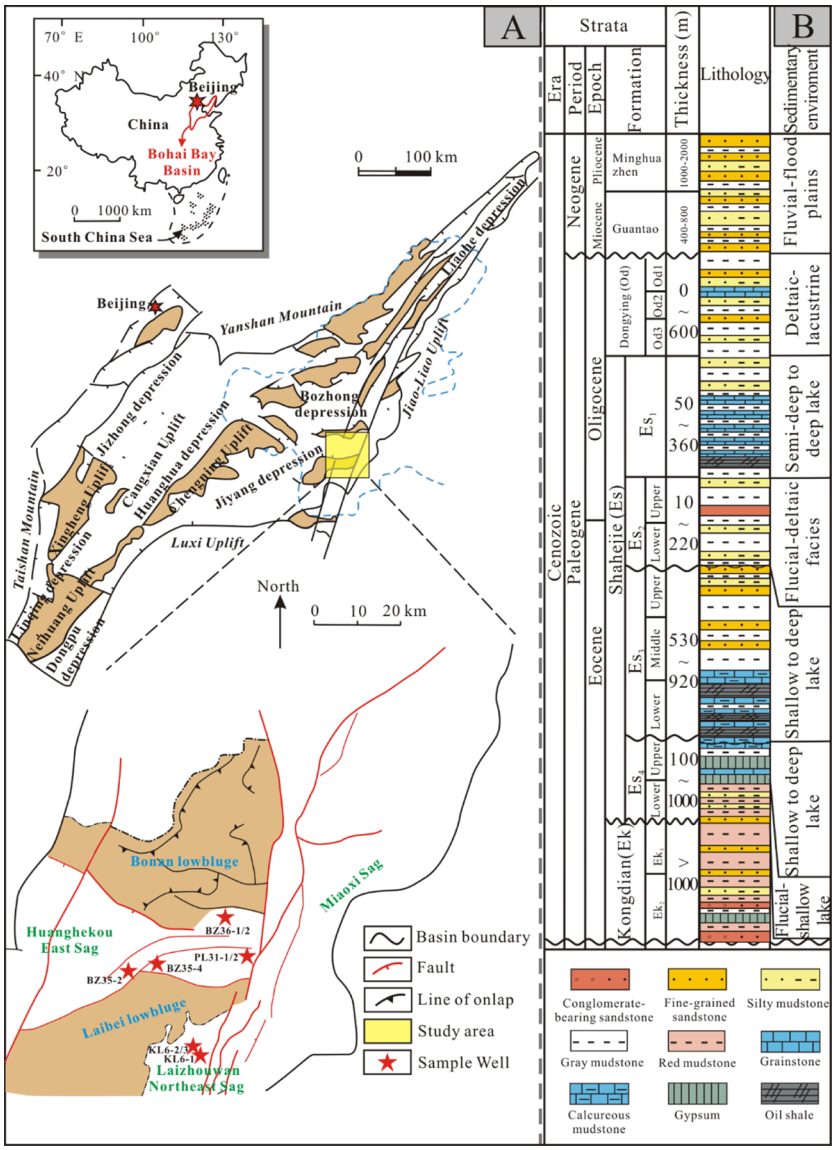


**Figure 1.** (a) Regional tectonic units of the Bohai Bay Basin, Huanghekou East Sag, and Laizhouwan Northeast Sag within the Bohai Bay Basin, structural units of the study area, and location of wells sampled here and (b) generalized lithology, stratigraphy, and depositional environment of the Bohai Bay Basin.

and *Rhodoplanes* spp.[46] Many novel hopanoids were reported following the development of technology. However, the origin and pathway of the diagenetic evolution of some novel hopanoids are obscure. Clearly, a deeper understanding of the fate of hopanoids during diagenesis needs more data from field and laboratory studies.

Compound-specific isotope analysis is the effective method to distinguish the organic matter with specific sources including chlorophyll, cuticular waxes, and bacteria.[47−49] Stable carbon isotopic fractionation may be determined by the origin and fate of some compounds in the sedimentary environment.[50,51] Compound-specific isotope analysis has been used for oil−oil and oil−source correlations.[52,53] The carbon isotope of an individual hopane has been reported to have a special origin, including homohopane, homohop-17(21)-enes, benzohopanes, neohop-13(18)-enes, and aromatized hopanoids.[14,24,54−56] Thermal maturation, depositional environment, and mixture of generated hydrocarbons might stymy the source analysis of petroleum.[49] However, the fractionation effects in diagenetic reactions likely impact the carbon isotope values of the precursor molecules.[51]

Abundant hopanoids including hopanes, secohopanes, benzohopanes, aromatized secohopanes, and sulfide hopanes were identified in a suite of low-maturity crude oils from the Huanghekou East Sag and the Laizhouwan Northeastern Sag. Therefore, the analysis of the evolution of hopanoids under reducing lacustrine environments is possible in the study area. The aims of this study are to show the origin of hopanoids in reservoir oils using compound-specific carbon isotopic analysis to illustrate the fate of hopanoids sourced from different depositional environments and to predict the coeval growing environment of the dominant aquatic microorganism.

## 2. GEOLOGICAL SETTING

Bohai Bay Basin in East China (Figure 1) is among one of the most petroliferous basins, with an area of about $4.2 \times 10^4$ km$^2$.[57,58] The Bohai Bay Basin is an intracratonic rift basin that has experienced two major tectonic evolution stages including


https://doi.org/10.1021/acsomega.1c02762
ACS Omega 2021, 6, 30298−30314

Table 1. Biodegradation Level and Bulk Geochemistry Characteristics of the Investigated Lacustrine Oils from Bohai Bay Marginal Sags

| | | | | | | fractions content (%) | | | |
|---|---|---|---|---|---|---|---|---|---|
| sample ID | depth (m) | formation | PM level | sulfur content (%) | bulk oils $\delta^{13}C$ (‰) | saturates | aromatics | resins | asphaltenes |
| Laizhouwan Northeastern Depression | | | | | | | | | |
| KL6-1 | 1374.5−1440 | $N_1m^L$ | 2 | nd | −26.3 | 57.58 | 26.26 | 8.85 | 3.23 |
| KL6-2 | 2153−2181 | $E_3d_2^L$ | 1 | 0.31 | −27.4 | 60.00 | 20.26 | 10.77 | 2.56 |
| KL6-3 | 2561−2565 | $E_3s_2$ | 1 | 0.4 | −27.3 | 57.35 | 20.41 | 13.47 | 3.47 |
| KL6-4 | 2585−2603 | $E_3s_2$ | 1 | 0.52 | −27.6 | 56.30 | 21.75 | 13.01 | 6.10 |
| Huanghekou Eastern Depression | | | | | | | | | |
| BZ35-2 | 2685.5−2703.5 | $E_3d_3$ | 1 | 1.4 | −26.8 | 41.75 | 24.50 | 15.00 | 17.25 |
| BZ35-3 | 2912.2−2930 | $E_3s_2$ | 1 | nd | −26.6 | 65.15 | 16.92 | 7.58 | 14.65 |
| BZ36-1 | 1297−1321.5 | $N_1m^L$ | 5 | 2.95 | −26.8 | 32.38 | 37.14 | 14.29 | 9.52 |
| BZ36-2 | 1552−1570 | $N_1g$ | 2 | 2.07 | −26.5 | 37.17 | 34.87 | 15.46 | 7.24 |
| PL31-1 | 1507−1529.5 | $N_1g$ | 3 | 1.12 | −26.1 | 46.10 | 30.50 | 11.35 | 4.61 |
| PL31-2 | 1241.5−1259 | $N_1g$ | 5 | 1 | −26.1 | 43.62 | 36.38 | 14.47 | 2.77 |
| BZ35-4 | 2449−2468.5 | $E_3d_2^L$ | 1 | 0.57 | −26.2 | 58.53 | 24.04 | 10.46 | 3.30 |

the Paleogene syn-rift stage and the Neogene-Quaternary post-rift stage.[59,60] A series of grabens and half-grabens developed along major NW- and NE-trending fault sets during the syn-rift stage.[61,62] Three sedimentary sequences from bottom to top include the Paleogene Kongdian Formation (Ek), the Shahejie Formation (Es), and the Dongying Formation (Ed), which were deposited in the syn-rift stage (65−24.6 Ma).[63,64] During the post-rift stage, the whole basin experienced a thermal subsidence, and the sedimentary sequences consist of the Neogene Guantao Formation (Ng), the Minghuazhen Formation (Nm), and the Pingyuan Formation (Qp) from bottom to top.[65]

The Huanghekou East Sag and the Laizhouwan Northeastern Sag are located in the south area of the Bohai Sea.[29,66,67] The two sags are separated by the Laibei low uplift and are controlled by NNE and NWW-EW striking extension faults.[68] The Huanghekou Sag is one of the margin sags in the Bohai Bay Basin and is a typical fault depression with a north fault and a south slop, which is bunded by structural units including the Bonan low uplift to the north, the Miaoxi South Sag, and the Laibei low uplift to the east and south.[69] The west branch of the Tanlu Fault passes through the middle of the Huangkekou Sag, separating the sag into the west sag and the east sag (Figure 1). The Palaeogene and Neogene strata are composed of the Ek, Es, Ed, Ng, and Nm in younger ages, of which Es and Ed are excellent-quality source rocks.[69] The good-quality source rocks in the Huanghekou East Sag are mainly controlled by tectonic, paleo-climate, paleo-productivity, and preservation condition of the organic matter.[69] The hot and humid climate is interpreted to cause the high level of productivity of algae and relative high organic contents in the source rocks in $Es_3$ in a semideep to deep lake environment. The $Es_{1-2}$ source rocks are deposited in the environment of lower temperatures and are associated with algal blooming and have a high level of paleo-productivity. The $Ed_L$ source rocks with mixed sources of organic matter including algal and terrigenous plant matter are deposited in a warm and semihumid climate.[69] The reducing environments are in favor of the preservation of organic matter.[69] The Laizhouwan Northeastern Sag is also a typical marginal sag and it is formed by the uplift during the Ek-$Es_4$ stages.[70] The fluctuation of subsidence and uplift after the $Es_4$ stage results in large amounts of deposits, including $Es_3$, $Es_2$, $Es_1$, and Ed.[70] The organic sources of the $Es_3$ member are mainly lower aquatic organisms and prokaryotes. The bottom water conditions fluctuate among the stratified, anoxic conditions and freshwater, weak reducing conditions.[71] The organic matter in the $Es_2$ member is derived from less aquatic organisms in more saline and anoxic bottom water than that in the $Es_1$ member.[71] Shales in the $Ed_3$ member are characterized by abundant terrigenous organic matter in the less saline and weaker reducing depositional conditions.[71]

## 3. SAMPLES AND METHODS

Full details have been reported elsewhere[72] but are summarized as follows.

**3.1. Samples.** A suite of 11 crude oils were analyzed in this study (Table 1). Four samples were from the Laizhouwan Northeasten Sag and seven samples were from the Huanghekou East Sag. A detailed analysis of aliphatic hydrocarbons was presented in the study of Niu et al.[72]

The samples obtained from the Laizhouwan Northeastern Sag were slightly biodegraded, corresponding to level 1 based on the Peters and Moldowan[6] biodegradation scale (abbreviated as PM 1). The sulfur contents of these oils were lower than 0.5%. There were five high sulfur oils (HSOs: BZ35-2, BZ36-1, BZ36-2, PL31-1, and PL31-2) and two low sulfur oils (LSOs: BZ35-3 and BZ35-4) obtained from the Huanghekou East Sag (Table 1). The HSOs experienced a slight to heavy biodegradation with the PM level from 1 to 5, while LSOs were on PM level 1.

Isorenieratane was identified in HSOs, illustrating a photic zone euxinic paleoenvironment.[73] Meanwhile, the Gammacerane index (0.08−0.23, average 0.16), $C_{35}S/C_{34}S$ hopane (0.79−1.10, average 0.91), and the ETR index (0.36−0.44, average 0.40) of HSOs represented brackish and saline water conditions. Furthermore, the organic matter mainly originated from algae and bacteria, and the maturity of all samples was in the low-mature to mature stage according to the identification of aliphatic biomarkers.[72]

**3.2. Separation of Aliphatic Hopanes, Benzohopanes, Secohopanes, and Sulfidic Hopanes.** The details of the separation methods of aliphatic hopanes, benzohopanes, secohopanes, and sulfidic hopanes were described by Cheng et al.,[74] Jiang et al.,[75] Wang et al.,[76] and Wu et al.,[77] respectively. The methods were introduced briefly in the following.



https://doi.org/10.1021/acsomega.1c02762
ACS Omega 2021, 6, 30298−30314

The hopanes were mainly separated from the aliphatic fractions. First, the asphaltene was precipitated with excess *n*-hexane, and then the maltenes were separated into aliphatic and aromatic fractions and resins by column chromatography with *n*-hexane, *n*-hexane:dichloromethane (1:2, V/V), and dichloromethane as rinsing solvents, respectively. The column chromatograph (15 cm length and 6 mm i.d.) was filled with activated alumina. The alumina (neutral, 100−200 mesh) were activated at 450 °C for 5h. The saturated fraction was further separated into purified *n*-alkanes and branched/cyclic alkanes by urea adduction. The hopanes were all enriched in the second fraction for the analysis of individual carbon isotopes.

The benzohopanes and aromatic secohopanes were all enriched in the monoaromatic fraction. A total of aromatic hydrocarbons (ca. 1−10 mg) in a minimum volume of *n*-hexane were carefully introduced to the top of the prepared column chromatograph (15 cm length and 6 mm i.d.) over activated alumina (450 °C for 5h). The sample container was rinsed three times with 100 μl *n*-hexane to fully transfer the aromatic hydrocarbons into the column. Then, *n*-hexane:dichloromethane (99:1, V/V, 5.5mL) was used to elute the monoaromatic hydrocarbons. Because of the volatility of the reagents, this experiment was best carried out at a room temperature of 25 °C.

The sulfide hopanes were separated by the methylation−demethylation method. Briefly, the crude oils (1 g) were dissolved in 5 mL of dichloromethane, and silver tetrafluoroborate (5 mol equiv) and methyl iodide (5 mol equiv) were added into the solvent. After that, the solution was stirred in the dark at room temperature for 24 h. The reaction products were centrifuged to separate the supernatant and precipitates, and the precipitates were removed by filtrating and evaporating dichloromethane using a rotating evaporator. The oily residue was mixed with 10 mL of *n*-hexane and kept in a refrigerator. Sulfonium salts were isolated by decanting the *n*-hexane supernatant after precipitation and centrifugation, and this procedure was repeated three times. The sulfonium salts were dissolved in 5 mL of acetonitrile and 10 mol equiv of 7-azaindole was added afterward, and then the solution was stirred in darkness for 24 h. The thiophenic fraction was extracted via *n*-hexane (10 mL, 3 times). 10 mol equiv of 4-dimethylaminopyridine was added to the residue and refluxed for 12 h. The sulfidic fraction was extracted by *n*-hexane (10 mL, 3 times).

**3.3. Gas Chromatography−Mass Spectrometry Analysis.** GC was performed on an HP6890 gas chromatograph equipped with a DP-5 MS-fused silica column (60 × 0.25 m i.d. and film thickness 0.25 μm) coupled to an HP 5973 mass selective detector (the ionization source operates at an electron beam energy of 70 eV). The aliphatic and aromatic fractions were analyzed in the same program in which the column was held at 40 °C for 2 min, which was then increased to 310 °C at 4 °C/min, with a final hold of 20 min. The program of sulfidic fractions was the same as that of saturate fractions, but the final hold was extended to 40 min. Helium was used as the carrier gas at a constant flow rate of 1.0 mL/min.

**3.4. Gas Chromatography−Isotope Ratio Mass Spectrometry.** Carbon isotopic analyses of *n*-alkanes, isoprenoids, and monoaromatic hydrocarbons were performed on a Thermo Scientific Delta V Advantage stable isotope ratio mass spectrometer system interfaced to a Trace Ultra gas chromatograph (Thermo Scientific; J&W DB-5 fused silica column: 30 × 0.25 m i.d. and 0.25 μm film thickness). The GC oven temperature for the analysis of isotopic hydrocarbons was initially held at 50 °C for 2 min and increased to 310 °C at 1 °C/min, with a hold of 20 min. The GC oven temperature for the analysis of monoaromatic hydrocarbons was held at 50 °C for 2 min, increased to 290 °C at 2 °C/min, and then ramped to 310 °C at 1 °C/min, with a final hold of 20 min. The temperature of the isotope ratio mass spectrometry oxidation oven was 1000 °C. A standard mixture of *n*-alkanes with known $^{13}C$ isotope values was analyzed over five samples to check the accuracy of the instrument. The isotopic compositions of all samples were relative to VPDB and were determined at least twice with a standard deviation for *n*-alkanes of ±0.8‰.

## 4. RESULTS

**4.1. Hopanes in the Aliphatic Fraction.** *4.1.1. Hopanes.* Hopanes are derived from bacterial membrane precursors and are widely distributed in sediments and petroleum.[78−80] The integrated distribution of hopanes is shown in Figure 2. $C_{30}$ 17α(H), 21β(H) hopane is the dominant compound among its homologues. Hopanes range from $C_{27}$ to $C_{35}$ without $C_{28}$. The abundance of $C_{35}$ hopanes in HSOs is obviously higher than that of LSOs. Meanwhile, a higher gammacerane index of HSOs suggests stratification of the sedimentary water body.[80] In addition, the abundance of 17α(H)-22,29,30-trinorhopane (Tm) in all samples is higher than that of 18α(H)-22,29,30-trinorneohopane (Ts), indicating the low-mature stage of the samples.

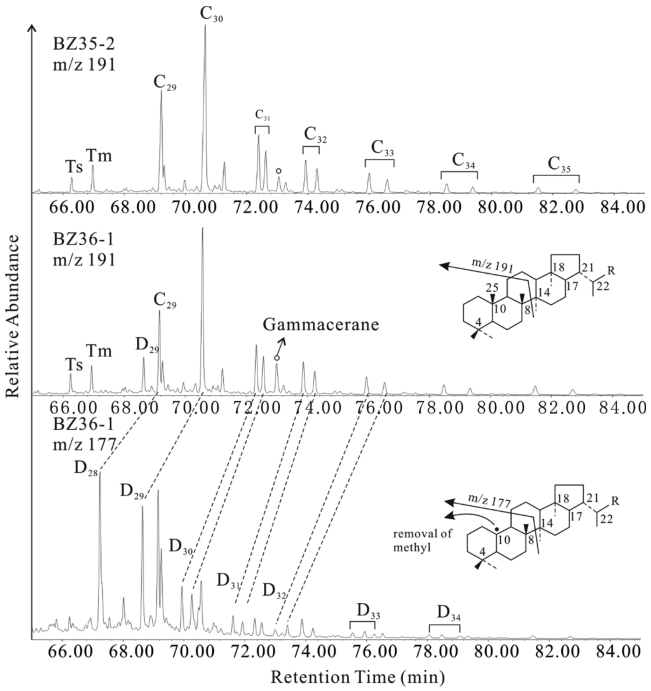


**Figure 2.** Representative mass chromatograms (*m/z* 191 and 177) showing the distribution of hopanes and 25-norhopanes in BZ35-2 and BZ36-1 samples. Ts: 8α(H)-22,29,30-trinorneohopane; Tm: 17α(H)-22,29,30-trinorhopane; $C_{29}$−$C_{35}$: $C_{29}$−$C_{35}$ hopanes; $D_{28}$-$D_{34}$: $C_{28}$−$C_{34}$ 25-norhopanes.

Hopanes are more resistant to biodegradation than *n*-alkanes, isoprenoids, and bicyclic sesquiterpanes.[74] In heavily degraded oils, demethylation of hopanes occurs to form 25-norhopanes.[15,81] The 25-norhopanes are identified in the


https://doi.org/10.1021/acsomega.1c02762
ACS Omega 2021, 6, 30298−30314

Table 2. Carbon Isotope of Hopanoids[a]

| sample ID | $C_{29}H$ (‰) | $C_{30}H$ (‰) | (22S + 22R) $C_{31}H$ (‰) | $D_{29}H$ (‰) | $C_{32}BH$ (‰) | $C_{33}BH$ (‰) | $C_{34}BH$ (‰) | $C_{35}BH$ (‰) | $C_{29}SH$ (‰) | $C_{30}SH$ (‰) |
|---|---|---|---|---|---|---|---|---|---|---|
| Laizhouwan Northeastern Depression | | | | | | | | | | |
| KL6-1 | −37.44 | −35.21 | nd | nd | nd | nd | nd | nd | nd | nd |
| KL6-2 | −37.49 | −37.74 | −38.66 | nd | −35.27 | −36.00 | −32.65 | −32.15 | −44.65 | −44.99 |
| KL6-3 | −33.90 | −34.34 | nd | nd | nd | nd | nd | nd | nd | nd |
| KL6-4 | −38.05 | −38.53 | nd | nd | nd | nd | nd | nd | nd | nd |
| Huanghekou Eastern Depression | | | | | | | | | | |
| BZ35-2 | −33.93 | −36.33 | −37.28 | nd | −32.01 | −32.39 | −30.96 | −35.58 | −43.94 | −43.26 |
| BZ35-3 | −33.38 | −31.47 | −34.00 | nd | nd | nd | nd | nd | −41.15 | −42.27 |
| BZ36-1 | −37.44 | −37.56 | −36.77 | −35.71 | −31.27 | −32.98 | −34.22 | −35.28 | −45.60 | −42.77 |
| BZ36-2 | −35.41 | −35.12 | −37.88 | | −32.41 | −32.04 | −31.38 | −32.80 | −44.06 | −42.77 |
| PL31-1 | −35.06 | −35.93 | −35.78 | −35.79 | −31.34 | −31.31 | −31.31 | −30.88 | nd | nd |
| PL31-2 | −37.59 | −36.99 | −35.40 | nd | nd | nd | nd | nd | nd | nd |
| BZ35-4 | −34.66 | −33.88 | −36.62 | nd | −31.80 | −31.95 | −30.63 | −32.18 | −43.90 | −43.56 |

[a]$C_{29}H$: $C_{29}$, 17$\alpha$, 21$\beta$ (H)-hopane; $C_{30}H$: $C_{30}$, 17$\alpha$, 21$\beta$ (H)-hopane; (22S + 22R) $C_{31}H$: (22S + 22R), $C_{31}$, 17$\alpha$, 21$\beta$ (H)-hopane; $D_{29}H$: $C_{29}$, 25-norhopane; $C_{32}BH$: $C_{32}$, benzohopane; $C_{33}BH$: $C_{33}$, benzohopane; $C_{34}BH$: $C_{34}$, benzohopane; $C_{35}BH$: $C_{35}$, benzohopane; $C_{29}SH$: $C_{29}$, 8,14-D-ring monoaromatic secohopane; $C_{30}SH$: $C_{30}$, 8,14-D-ring monoaromatic secohopane; nd = not determined.

heavily biodegraded oils including PL31-2 and BZ36-1, suggesting that 25-norhopanes are formed by microbial demethylation of hopanes. In this study, a minor peak of $C_{29}$ 25-norhopane ($D_{29}$) can be observed in the $m/z$ 191 mass chromatogram, and hopanes could be identified in the $m/z$ 177 mass chromatogram of PL31-2 and BZ36-1, suggesting incipient biodegradation of hopane compounds.[74]

In order to determine potential diagenesis relationships, the $^{13}C$ isotope values of the series of hopanes and 25-norhopanes are measured (Table 2). The $^{13}C$ isotope values of $C_{29}$ and $C_{30}$ hopanes range from −38 to −31‰, while $\delta^{13}C$ values of most $C_{31}$ (22S + 22R) hopanes are more depleted than those of $C_{29}$ and $C_{30}$ hopanes, with the range of −39 to −33‰. On the contrary, in PL31-2 and BZ36-1, $^{13}C$ isotope values of 25-norhopanes are enriched in $^{13}C$ isotope values (−35.8 and −35.7‰, respectively).

*4.1.2. 8,14-Secohopane.* Isomers of 8,14-secohopanes can be identified (Figure 3) by comparing the relative retention time and mass spectra in previous studies.[82,83] All of these marked peaks in these chromatograms represent compounds with mass spectra containing a base peak of $m/z$ 123 and a molecular ion appropriate for secohopanes. The $C_{29}$ and $C_{30}$ 8,14-secohopanes are recognized by the molecular ions at $m/z$ 400 and 414 and $m/z$ 123, 193, and 267 fragment ions. The mass spectra of $C_{29}$ and $C_{30}$ 8,14-secohopanes are listed in the Supporting Information (Figure S1a,b). Furthermore, six pseudohomologous series extending to $C_{35}$ are identified mainly by the molecular ion at $m/z$ 428, 442, 456, 470, and 484 and the base peak at $m/z$ 191. These compounds can be classified into secohopanes and secomoretanes. Owing to the ring C opening, some novel 8,14-secohopanes configured at the C-8, C-14, C-17, and C-21 positions are found. In most cases, the peaks occur as pairs from $C_{31}$ to $C_{35}$ presumably because of the occurrence of diastereomers due to the chiral center at $C_{22}$.[83] Therefore, the abundances of 8$\alpha$, 14$\alpha$, 17$\alpha$, 21$\beta$(H)-secohopanes and 8$\alpha$, 14$\beta$, 17$\beta$, 21$\alpha$(H)-secomoretanes are higher than other counterparts.

**4.2. Hopanes in the Aromatic Hydrocarbon Fraction.** *4.2.1. Benzohopanes.* Benzohopanes are separated from monoaromatic fraction, showing a relatively high abundance (Figure 4). These $C_{32}$−$C_{35}$ benzohopanes are suggested to be formed by the side-chain cyclization at $C_{20}$, followed by the aromatization.[84,85] They occur widely in high abundances in sedimentary rocks and crude oils in carbonate-rich and evaporitic environments.[33,84,85] The $C_{32}$−$C_{35}$ benzohopanes with distributions similar to those of $C_{32}$−$C_{35}$ hopanes have the same base peak at $m/z$ 191 with molecular ions at $m/z$ 432, 446, 460, and 474. The mass spectra of benzohopanes are listed in the Supporting Information (Figure S1c−f). However, the $^{13}C$ isotope values of benzohopanes vary from −36 to −31‰ (Table 2) and are more enriched than hopanes.

Benzohopanes may be ubiquitous components, especially abundant in confined and reducing environments.[86,87] The predominance of the $C_{34}$ counterpart among benzohopanes has been reported in evaporitic rock samples; however, the carbon isotope depletion of $C_{32}$ to $C_{35}$ benzohopanes in oils is tentatively attributed to migration effects of hydrocarbons.[84]

*4.2.2. D-Ring Monoaromatic SHs, DSHs, and IDs.* The isomers of 8,14-secohopanoids (SHs), D-ring monoaromatic 8,14-Seco-28-nor-hopanoids (DSHs), and indenyldrimanes (IDs) are identified in the $m/z$ 365, 351, and 363 mass chromatograms by comparison of the relative retention time with those in the literature studies.[87,88] The $m/z$ 365, 351, and 363 mass chromatograms show the monoaromatic fraction from the oil sample in well BZ35-2 (Figure 4). SHs have abundant $C_{29}$ and $C_{30}$ compounds, while the abundance of $C_{31}$ SH is in minute abundance. The $^{13}C$ isotope values of $C_{29}$ and $C_{30}$ SHs vary from −45 to −41‰ (Table 2), which is more depleted than that of hopanes and benzohopanes. DSHs are the demethylated counterparts of regular SHs.[87] The $C_{29}$ DSH is the dominant constituent in DSHs and the peaks of $C_{28}$ to $C_{30}$ DSHs occur as pairs. IDs at $m/z$ 363 are a series of aromatic secohopanoids in oils, which are counterparts of the regular SHs but containing an extra C═C bond in the E-ring.[87] The typical mass spectra of SHs, DSHs, and IDs are listed in the Supporting Information (Figure S1(g−l)).

**4.3. Hopanes in Sulfidic Fraction.** A homologous series of hexacyclic sulfides with a 17$\alpha$, 21$\beta$(H) hopane carbon skeleton ranging from $C_{30}$ to $C_{35}$ are identified by Cyr et al.[36] in heavy oils of Northern Alberta. Schaeffer et al.[37] described the structural elucidation of sulfide hopanes and separated them into eight series. By comparing with the relative retention time and mass spectra,[37] the structures of compound-1 and compound-2 are represented in Figure 5a. The mass spectra


https://doi.org/10.1021/acsomega.1c02762
ACS Omega 2021, 6, 30298−30314

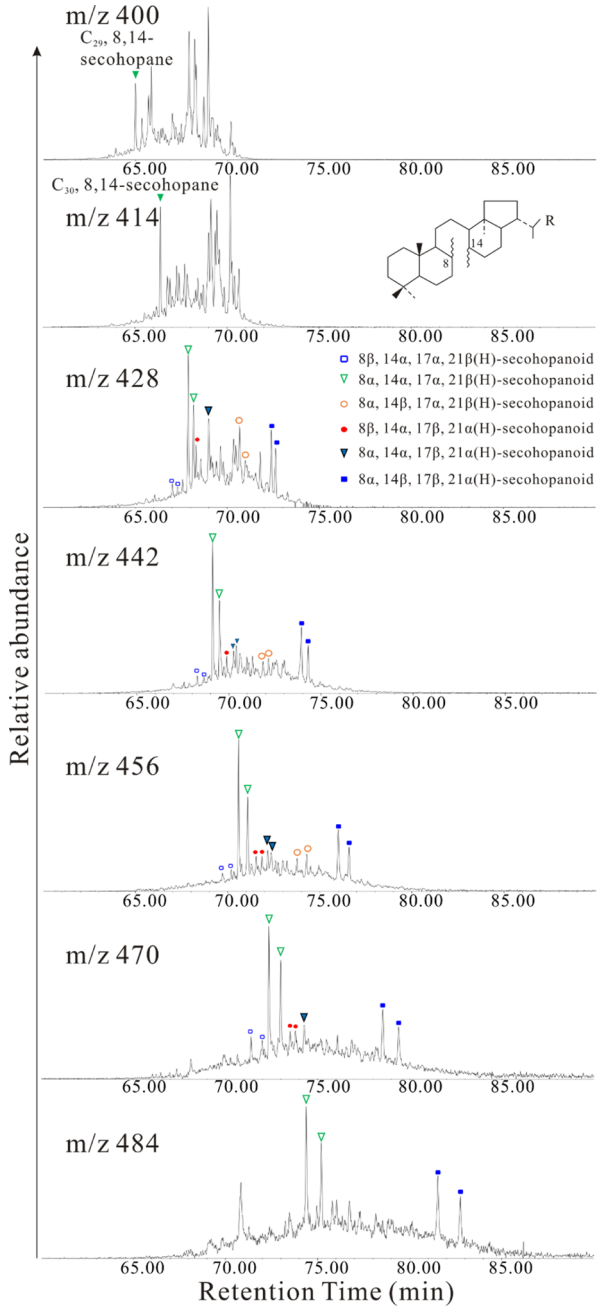


**Figure 3.** Representative mass chromatograms showing the distribution of 8,14-secohopanes from $C_{29}$ to $C_{35}$ in BZ35-2 samples.

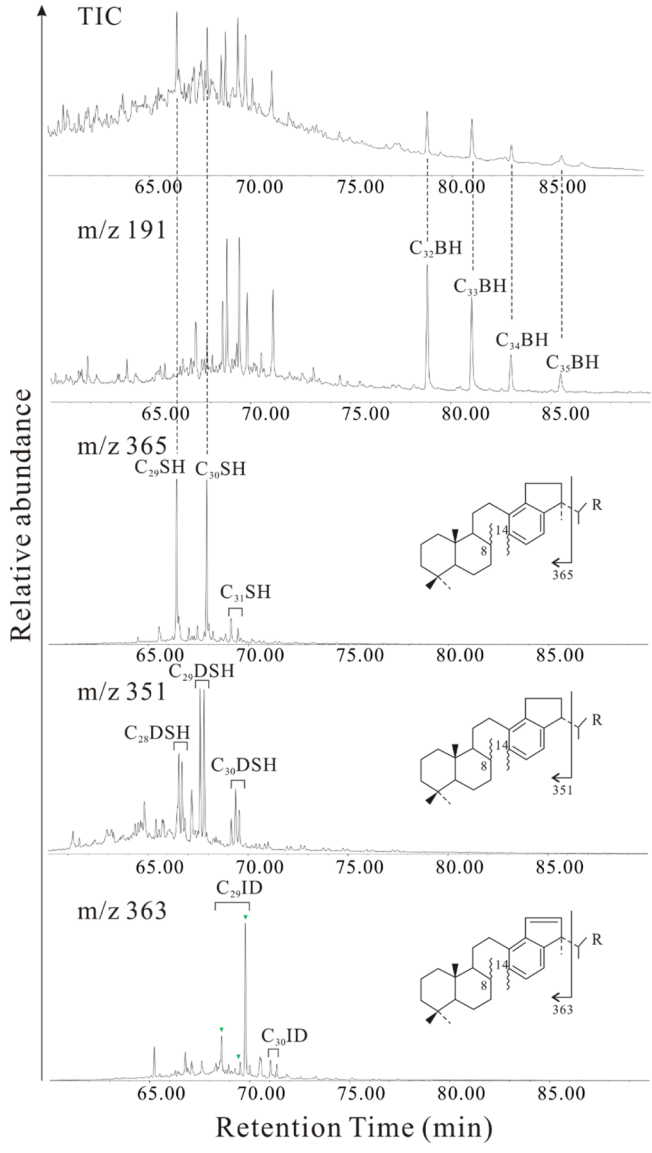


**Figure 4.** Representative mass chromatograms showing the distribution of benzohopanes (*m/z* 191), D-ring monoaromatic 8,14-secohooanoids (*m/z* 365), D-ring monoaromatic 8,14-seco-28-norhopanoids (*m/z* 351), and indenyldrimanes (*m/z* 363) in aromatic hydrocarbon of BZ35-2 samples.

are listed in the Supporting Information (Figure S1m−p). The spectra of the sulfides from these compounds show a base peak at the molecular ion and doublets of fragments at *m/z* 191 and *m/z* 235 ($C_{31}$ homologue) + 14*n* due to the cleavage of ring C. The mass spectra of compound-1 and compound-2 (Figure S1m-p) show similarities; however, the presence of a fragment at *m/z* 122 in compound-2 with a higher intensity than in the case of compound-1 is a typical feature of these compounds.[37]

A compound with a base peak at *m/z* 395 is co-eluted with compound-1 of $C_{32}$ sulfide hopane ($C_{32}$SH-1, Figure 5b), resulting in a relatively high abundance of $C_{32}$SH-1. As shown in the mass spectrum of $C_{32}$SH-1 (Figure S1o), the fragments at *m/z* 395 and the molecular ion (*m/z* 484) are similar to the mass spectrum of compound B (Figure 5d), suggesting the co-elution of $C_{32}$SH-1 and compound B. The mass spectrum of $C_{32}$SH-2 is shown in Figure S1p, suggesting that $C_{32}$SH-2 is less influenced.

The mass spectra of compounds A−E are shown in Figure 5c−g. The spectra of these compounds show a base peak at *m/z* 395 and fragments at *m/z* 121, *m/z* 163, *m/z* 191, and *m/z* 75 (compound A homologue) + 14*n* ($0 \leq n \leq 4$). Compounds from A to E show molecular ions from $M^+$ 470 to 526. More details about the structure of these compounds are beyond the scope of this paper, which needs further study in future studies.

## 5. DISCUSSION

**5.1. Sources of Hopanes.** An important source of high-molecular-weight hopanoids (>$C_{30}$) is from the diagenetic transformation of bacteriohopanepolyols in membrane lipids in a wide range of prokaryotes including cyanobacteria and heterotrophic and methanotrophic bacteria.[18,23,89] In addition, lower pseudohomologues ($C_{30}$ or less) may be related to their


https://doi.org/10.1021/acsomega.1c02762
ACS Omega 2021, 6, 30298−30314

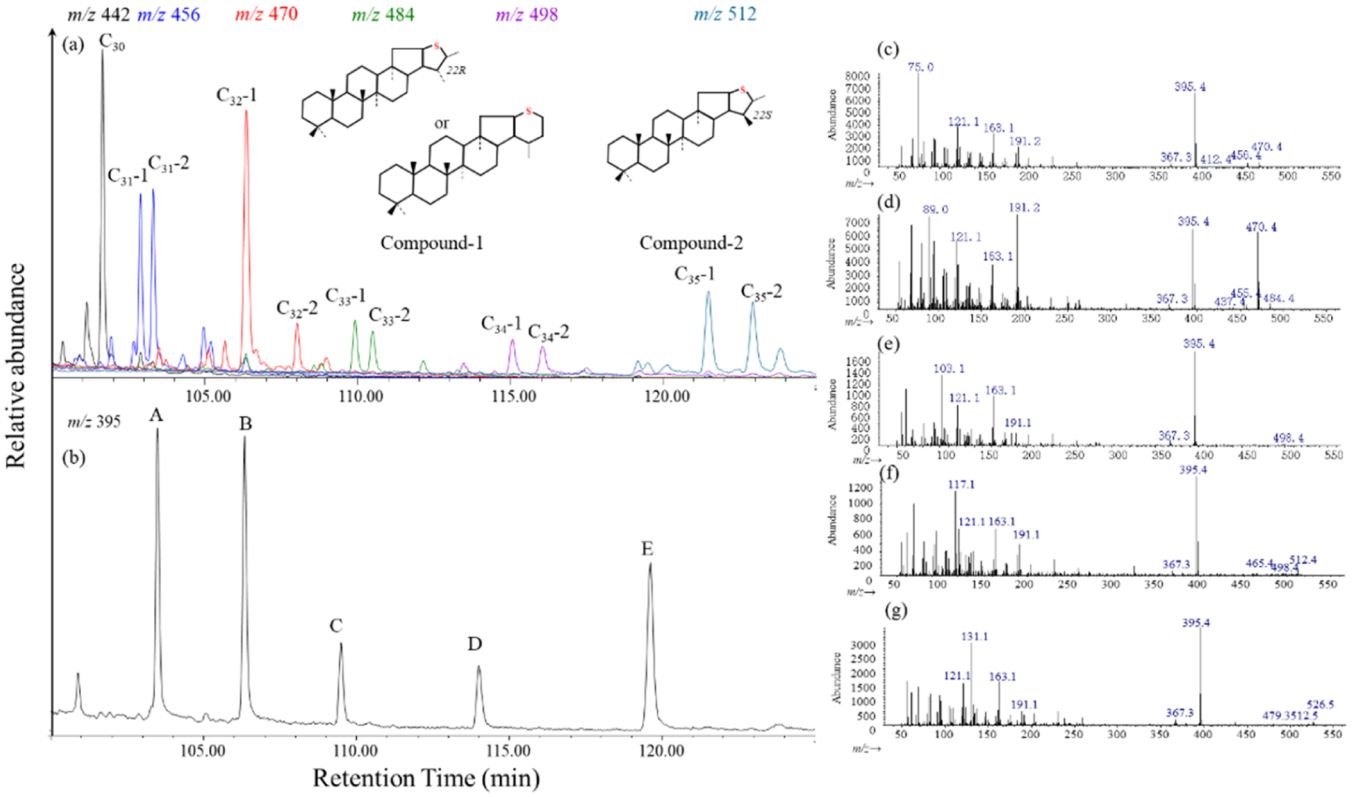


**Figure 5.** Representative mass chromatograms showing the distribution of sulfide hopanes from $C_{30}$ to $C_{35}$ in sulfide fractions of BZ35-2 samples, $C_x$-1: compound-1 of $C_x$ sulfide hopane and $C_x$-2: compound-2 of $C_x$ sulfide hopane (a); mass chromatograms showing the distribution of compound A to compound E in sulfide fractions of BZ35-2 samples (b); mass spectra of compound A to compound E (c–g).

$C_{30}$ precursors such as diplopterol (hopan-22-ol) or diploptene (hop-22(29)-ene), found in nearly all hopanoid-producing bacteria.[28,33,90,91] Hopanoids were once thought as biomarkers of aerobic bacteria (Talbot and Farrimond[23] and references therein) even though their biosynthesis does not require $O_2$. However, the biosynthesis of the hopanoids has now been reported in a series of anaerobic bacteria.[42,92] Therefore, abundant hopanes found in aliphatic, aromatic, and sulfidic fractions might imply that their diagenetic environment may be closely associated with active microbial activities.

The $\delta^{13}C$ values of lipid biomarkers are strongly determined by the isotopic composition of their biosynthetic precursors and their biosynthesized pathway.[33,93] Generally, it is assumed that the carbon isotopic fractionation in a diagenetic process is limited.[51] The $^{13}C$ isotope value differences between $C_{31}$ hopane and $C_{29}$–$C_{30}$ hopanes ranging from −3.3 to 2.2‰ (Figure 6) might illustrate different bacterial sources of these compounds as these differences are larger than those from a single bacteriohopanepolyol precursor with a specific $^{13}C$ isotope value. There are abundant bacteriohopanepolyols with different chemical functional groups on the side chain, which are thought as potential indicators of various organisms. The differences in diagenetic transformation pathways result in the formation of homohopanes with different distributions.[14] The commonly occurring bacteriohopane-32,33,34,35-tetrol is ubiquitous in sediments and soils, and it is found in a diverse suite of microorganisms (Rohmer[19] and references therein). Therefore, it is not diagnostic for a specific bacterial community. It is ascertained that a wide range of $^{13}C$ isotope values between $C_{31}$ hopane and $C_{29}$–$C_{30}$ hopanes represent the different precursors of these compounds (Figure 6).

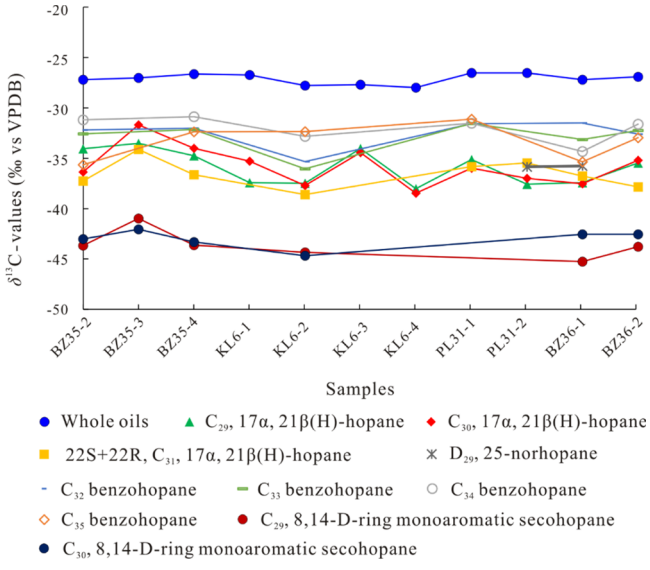


**Figure 6.** Distribution of the carbon isotopes of whole oils, hopanes, benzohopanes, and aromatic 8,14-secohopanes.

Diplopterol (hopan-22-ol) or diploptene (hop-22(29)-ene) was believed to be one of the precursors of a lower hopanoid (<$C_{30}$).[90] The $^{13}C$ isotope values of $C_{29}$ and $C_{30}$ hopanes may represent a similar origin, with the differences of $^{13}C$ isotope values from −0.8 to 0.7‰ in most samples. Oil samples in wells BZ35-2, BZ35-3, and BZ35-4 have greater differences of the $\delta^{13}C$ values between $C_{29}$ and $C_{30}$ hopanes. Sakata et al.[94] measured the carbon isotopic values of the cultured cyanobacterium Synechocystis UTEX 2470, finding that the


https://doi.org/10.1021/acsomega.1c02762
ACS Omega 2021, 6, 30298−30314

$^{13}C$ isotope values of $C_{30}$ diplopterol and diploptene are enriched (0.09−2.3‰) relative to that of bacteriohoptetrol. It is likely that the relative contribution of bacteriohopanetetrol and diplopterol (diploptene) leads to the fluctuation of $^{13}C$ isotope values between $C_{29}$ and $C_{30}$ hopanes in BZ35-2, BZ35-3, and BZ35-4 samples.

The 25-norhopane series, also named as 10-demethylhopanes, generally occur in biodegraded oils and are widely used to assess the biodegradation level.[6] The biological source of 25-norhopanes remains obscure. No microorganism is known to have the ability to biosynthesize 25-norhopanes.[15,73,96] The 25-norhopanes and their counterparts mostly in biodegraded reservoir oils indicate that 25-norhopanes originate directly from microbial degradation of hopanes.[74,81,96] However, the degradation compounds of hopanes are not only 25-norhopanes.[97,98] Intriguingly, no 25-norhopanes were observed in enrichment cultures or pure aerobic bacteria.[98] Methanogens living in fresh or brackish water were thought to be probably responsible for the degradation of hopanes to 25-norhopanes.[95,99] The 25-norhopanes were observed only in biodegraded oils (PL31-2 and BZ36-1 samples). However, no 25-norhopanes were detected in any of the *m/z* 177 of the non-biodegraded oils, perhaps indicating a major origin of microbial degradation. The $^{13}C$ isotope values of $C_{29}$ 25-norhopanes in PL31-2 and BZ36-1 are both higher than those of $C_{30}$ hopanes, with deviations of 1.1 and 1.8‰, respectively (Figure 6). It is likely that the 25-norhopanes are the microbially mediated demethylation products of hopanoids, which lead to the enrichment of the carbon isotopes. Dominance of the $C_{29}$ 25-norhopane suggests incipient biodegradation of hopane compounds.[74]

Benzohopanes were reported to be the transformation products of bacteriohopanetetrol.[84,85] Benzohopanes and $C_{31}$ hopane are both products of a transformation of bacteriohopanepolyol. Nevertheless, varying differences of $^{13}C$ isotope values (1.5−6.5‰) between these two types of hopanes might represent (1) the mediation of bacterial activities and (2) the enrichment of the $^{13}C$ isotope in the aromatization of these compounds. The $\delta^{13}C$ values of benzohopanes are even isotopically heavier than those of the $C_{29}$−$C_{30}$ hopanes and the $C_{29}$ 25-norhopane. Liao et al.[33] found $^{13}C$ enrichments of 2−4‰ in aromatized hopanes via diagenetic alteration and successive dehydrogenation from the D-ring to the A-ring. In our study, the $^{13}C$ isotope enrichment of some compounds is even greater than 5‰, suggesting that the benzohopanes are not only produced by cyclization of bacteriohopanepolyol, but they are also derived from heterotrophic or cyanobacteria in the paleo-ecosystem during deposition of its source rocks.[28] However, the cyanobacteria-derived biomarkers, such as the 2-methylhopanes[21] and 7-,8-monomethyl heptadecanes,[100] are absent in the samples, probably suggesting that cyanobacteria might have a minor contribution to the benzohopanes, perhaps indirectly indicating that the heterotrophic bacteria are responsible for the origin of the benzohopanes.

The D-ring-8,14-secohopanes in sedimentary organic matter have been reported for decades,[83,101−103] which might be formed in the subsurface from bacterial $C_{35}$ hopanoid precursors.[84] The heavily depleted $^{13}C$ isotopes (−45.6−41.2‰) of $C_{29}$ and $C_{30}$ SHs relative to hopanes and benzohopanes (Figure 6) tentatively suggest the mixed sources of SHs from methanotrophs and other bacteria.[103,104] Methanotrophs utilizing methane as the carbon source that produced depleted $\delta^{13}C$ values have been reported in previous research studies.[103,104] Freeman et al.[50] interpreted the heavily depleted carbon isotopes of hopanes (up to −65‰) as sources of various amounts of methylotrophs, that is, recycling of carbon through methanotrophs. Volkman et al.[18] reported a very light carbon isotope of $C_{29}$ hop-17(21)-ene (avg. −50.8‰) from an oil shale in the Huadian Basin, which was attributed to the contribution of methanotrophs. However, the $^{13}C$ isotopes of $C_{29}$ SH (−45.6−41.2‰) and $C_{30}$ SH (−45−42.2‰) are less depleted than hopanes with a sole methanotroph contribution, indicating the mixed input of some unknown bacterial sources and possibly the methanotrophs.[18,25] It is noteworthy that 3-methylhopanes are not the samples found in this study, which are similar to the methylhopanoids in the Huadian Basin, probably indicating that the original methanotrophs do not have the ability to biosynthesize 3$\beta$-methylhopanoids.[18]

**5.2. Diagenetic Factors Determining the Hopanoid Distributions.** The formation of hopanoids is controlled by multiple factors, such as bacterial degradation, diagenesis, thermal maturity, and biological precursors.[29,106]

Abundant sulfide hopanes are detected in HSOs (Figure 5). Due to the limited sulfur in microorganisms, the sulfur-containing compounds are thought to be formed by incorporated sulfur in functionalized hydrocarbons and carbohydrates under favorable water conditions.[107−109] There are two mechanisms of incorporating an inorganic sulfur element into organic matter. First, the molecules are synthesized via intermolecular sulfur bridges to form micromolecules, such as kerogen, asphaltenes, and resins.[110] Second, some functional groups in the molecules are added or substituted by inorganic reducing sulfur to form organic sulfur compounds with thiane, thiolane, and thiophene rings.[111] Cyr et al.[36] suggested that the predominant peaks of sulfide hopanes at *m/z* 442, 456, 470, 484, 498, and 512 were derived from hopanoids bearing either a thiacyclopentane ring between $C_{16}$ and $C_{21}$ or a thiacyclopentane ring between $C_{20}$ and $C_{21}$. The structures of sulfur hopanes are characterized by the linkage of the $C_{30}$ and the $C_{16}$ or the $C_{20}$ carbon position via a sulfur bond. In low-maturity samples, the sulfurization is closely associated with the bacterial sulfate reduction (BSR) and other reactions in early diagenesis.[112]

Numerous studies reported the isomerization and formation processes of hopanes.[14,18,25,91,113−117] A common sequence of reactions is conversion of bacteriohopanepolyol to hopene to hopane.[25] Nevertheless, rearranged hopanes and novel series of hopanes might have experienced the more complex transformation process under special conditions.[91,118] In this study, there is a dominance of normal hopane distributions. However, the 8,14-secohopanes occurring in saturated hydrocarbons might suggest the special generation mechanism for secohopanes. The 8,14-secohopanes are considered to be presumably derived from both hopanes and moretanes via ring C opening during maturation or degradation because the C-8,14 bond has the lowest energy in the whole hopane skeleton.[119] Wenger and Isaksen[103] reported that the 8,14-secohopanes were formed via a microbial alteration in the reservoir. Additionally, the compounds were directly formed during early diagenesis via transformation of bacteriohopanepolyol precursors,[106] with a high resistance to biodegradation.[103,120] The 8,14-secohopanes were recognized in all samples, including biodegraded and non-biodegraded oils. Further, the $C_{31}$−$C_{35}$ secomoretane/secohopane ratios have


https://doi.org/10.1021/acsomega.1c02762
ACS Omega 2021, 6, 30298−30314

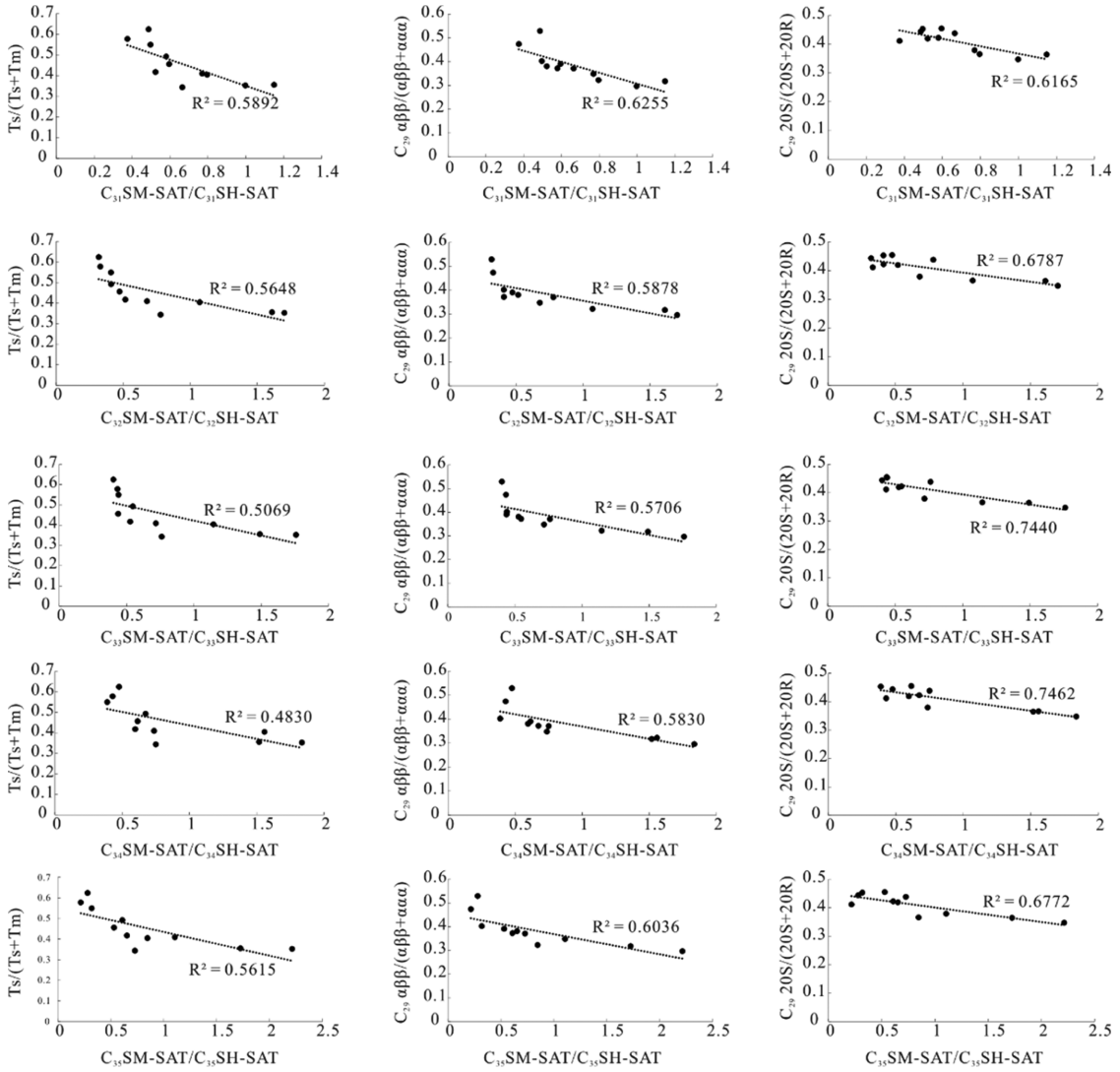


**Figure 7.** Correlations of $C_{31}$−$C_{35}$ SM-SAT/SH-SAT vs Ts/(Ts + Tm), $C_{29}$ $\alpha\beta\beta/(\alpha\alpha\alpha + \alpha\beta\beta)$, and $C_{29}$ 20S/(20S + 20R). $C_{31}$−$C_{35}$ SM-SAT: $C_{31}$−$C_{35}$ 8,14-secomoretanes in saturates. $C_{31}$−$C_{35}$ SH-SAT: $C_{31}$−$C_{35}$ 8,14-secohopanes in saturates.

negative correlations with thermal maturity parameters including Ts/(Ts + Tm), $C_{29}$ $\beta\beta/(\alpha\alpha + \beta\beta)$, and $C_{29}$ 20S/(20S + 20R) (Figure 7), suggesting the influence of maturity.

The benzohopanes are in high abundance in source rocks and crude oils under a reducing environment.[84,85] Besides cyclization at $C_{20}$, Schaeffer et al.[121] reported a novel series of benzohopanes cyclized at the $C_{16}$ position. These novel benzohopanes extending from $C_{31}$ up to $C_{35}$ and their mass spectra show a weak fragment at *m/z* 191 and a more pronounced *m/z* 197 + (*n* × 14). These benzohopanes always co-occur with the regular benzohopanes in immature sediments, particularly under carbonate-rich and evaporitic conditions.[33,121] However, benzohopanes in monoaromatic hydrocarbons have the base peak of *m/z* 191 with the corresponding molecular ions and the lack of $C_{31}$ compounds, suggesting that the benzohopanes are all regular counterparts. Regular benzohopanes are usually formed and enriched at the early diagenesis stage,[101,102] suggesting that the formation of compounds is not only influenced by thermal maturity but probably formed by the catalysis of the mineral matrix[84] or active microbial activities.[33] The enrichment of the $^{13}C$ isotope values might partly indicate that the diagenesis of these compounds is mediated by microbial reactions.

A series of SHs are particularly abundant in a confined environment[84] and are formed from bacteriohopanepolyols. However, the formation of aromatic 8,14-secohopanoids is likely to occur in the later stage of maturation.[102] Compared to benzohopanes, the formation of aromatic 8,14-secohopanes needs aromatization of the D ring and opening the C ring of original hopanoid molecules, which requires more energy in the later stage of oil window.[101,102] With an increase in maturity, SHs would convert to DSHs via demethylation and to IDs by further aromatization.[87] Both benzohopanes and aromatic 8,14-secohopanes are more resistant to biodegradation.[101] In view of the differences of formation and degradation between benzohopanes and aromatic 8,14-secohopanes, He and Lu[102] proposed a parameter, that is, D-ring monoaromatized 8,14-secohopanoids/(D-ring monoaromatized 8,14-secohopanoids + benzohopanes) (shortly, MAH) to evaluate the maturity of sediments and oils. It is suggested that the value of MAH at 0.3 may be the threshold of oil generation. However, in the low-mature oil samples, the MAHs are in the range of 0.83−0.94, which corresponds to the mature to high-


https://doi.org/10.1021/acsomega.1c02762
ACS Omega 2021, 6, 30298−30314

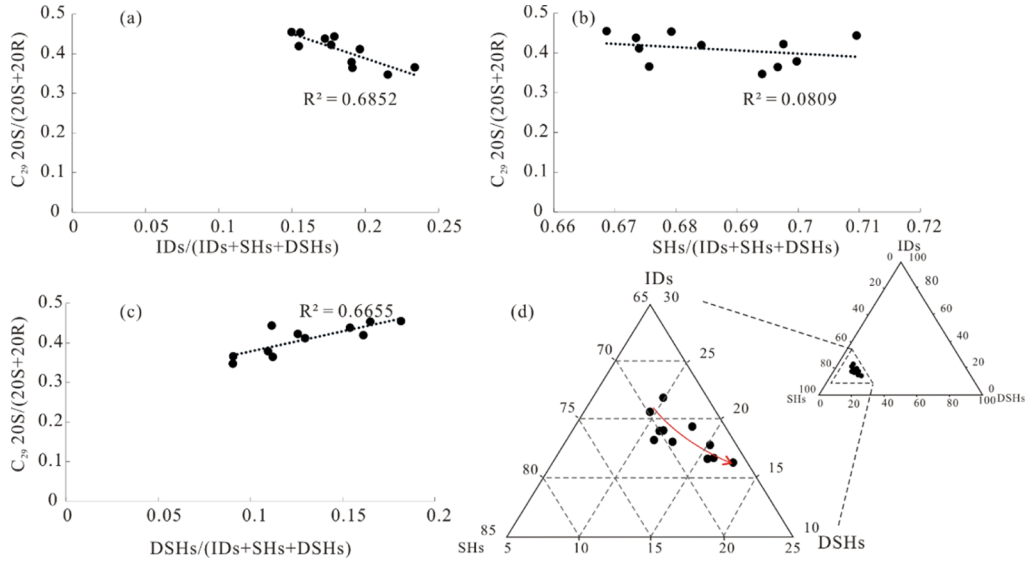


**Figure 8.** Correlations of $C_{29}$ 20S/(20S + 20R) vs IDs/(IDs + SHs + DSHs) (a), SHs/(IDs + SHs + DSHs) (b), DSHs/(IDs + SHs + DSHs) (c), and ternary diagram of IDs, SHs, and DSHs (d), showing the relative enrichment of IDs in low-mature samples.

mature stage based on He and Lu.[102] Therefore, the bacterial reaction of the compounds cannot be excluded. In addition, the relative distributions of SHs, DSHs and IDs are different from that reported in Killops et al.[87] In comparison with higher-maturity oils, there are abundant IDs in the relatively low-mature ones (Figure 8). This likely suggests that the formation of IDs might be mediated by microorganism reactions.[87,102] The prominent peaks of SHs, DSHs and IDs are $C_{30}$SH, $C_{29}$DSH, and $C_{29}$ID, respectively (Figure 4). The distribution of these compounds is similar to that of hopanes. However, a trace of aromatic 8,14-secohopanes (>$C_{30}$) is tentatively assigned in oils together with the depleted $\delta^{13}C$ values of $C_{29}$ and $C_{30}$ SHs, indicating the complexity of the diagenesis process and bacterial input. If methane is the main carbon source for the bacterial community, the $^{13}C$ isotope values of hopanoids and organic matter would be in the range of −70 to −90‰.[122] These results might imply that hopanoids from methanotrophs may have a contribution of SHs via microbial reactions during early diagenesis. Then, the $C_{30}$ precursor hopanoids are altered and formed the dominance of $C_{30}$SH in hopanes.

**5.3. Depositional Environment.** The high sulfur content and the identified abundant sulfur-containing hopanoids in HSOs together with isotopically depleted $C_{29}$ and $C_{30}$ SHs indicate that the depositional environment has an active carbon and sulfur cycle. The HSOs are mostly formed by the BSR and thermochemical sulfate reduction (TSR). TSR is proposed as the thermally driven reaction between a hydrocarbon and hydrogen sulfide.[123] The oils originated from the TSR reaction generally have high maturity and are rich in aromatic sulfur compounds including dibenzothiophenes and their derivatives.[124] This is obviously contradicted by our samples, which have abundant sulfide compounds formed by BSR in the low-maturity stage. A specific aryl isoprenoid, that is, isorenieratane, has been identified in the HSOs, implying the presence of sulfur bacteria in the photic zone euxinia of the water column.[125] Isorenieratane is exclusively biosynthesized by anaerobic, photosynthetic, green sulfur bacteria (Chlorobactene) living in organic-rich photic zones, where hydrogen sulfide is abundant for the generation of green sulfur bacteria.[126,127] The identification of isorenieratane and abundance of sulfur-containing compounds suggest the presence of sulfur-reducing bacteria and green sulfur bacteria (Chlorobactene) (Figure 9). In addition, abundant aryl isoprenoids are found in HSOs (Figure 9). Aryl isoprenoids are thought to be formed from the C−C bond cleavage of isorenieratene and $\beta$-isorenieratene with the isorenieratene from green sulfur bacteria, whereas $\beta$-isorenieratene was likely to be formed from the ubiquitous $\beta$-carotene.[126,128] Schwark and Frimmel[129] proposed the aryl isoprenoid ratio (AIR, $\Sigma C_{13-17}/\Sigma C_{18-22}$) to assess the persistence of photic zone euxinia. An AIR > 3.0 suggests a short-term episodic photic zone euxinic condition, while an AIR < 3.0 indicates persistent photic zone euxinia. Xu et al.[127] used isorenieratane/$C_{18}$ aryl isoprenoid (Iso/$C_{18}$) to evaluate the environment perturbations of $Es_4U$ member source rocks in the Dongying Depression. The source rocks in a marine setting usually have Iso/$C_{18}$ < 3.0, whereas marine-related events (such as summer hurricanes or the East Asian monsoon) may lead to an abrupt increase in the Iso/$C_{18}$ ratio. The AIR ranges from 0 to 0.8 (lower than 3.0) for HSOs, which probably implies a photic zone euxinic environment. This is consistent with the presence of isorenieratane in the photic zone euxinia of the water column. This hypothesis needs to be further investigated. Furthermore, the good correlation ($R^2$ = 0.86) between the sulfur content and the gammacerane index (Ga/$C_{30}$H) indicates that the reducing depositional environment partly results in the incorporation of an inorganic sulfur element into organic matters (Figure 10).

The sulfur-reducing bacteria can reduce the elemental sulfur to hydrogen sulfide, and the green sulfur bacteria would utilize it as an electron donor to oxidize it back to elemental sulfur.[130] The living conditions of green sulfur bacteria are an anaerobic and a transparent water column.[131] Isorenieratane is the diagenetic product of isorenieratene, which originates from brown pigmented *Chorobiaceae*.[131] Brown-pigmented green sulfur bacteria can adapt to the low irradiance and blooms of the bacteria occur at a 2−80 m depth of the water column (most water depths are less than 17m).[73] However, there is a low abundance of isorenieratane in HSOs. The three possible


https://doi.org/10.1021/acsomega.1c02762
ACS Omega 2021, 6, 30298−30314

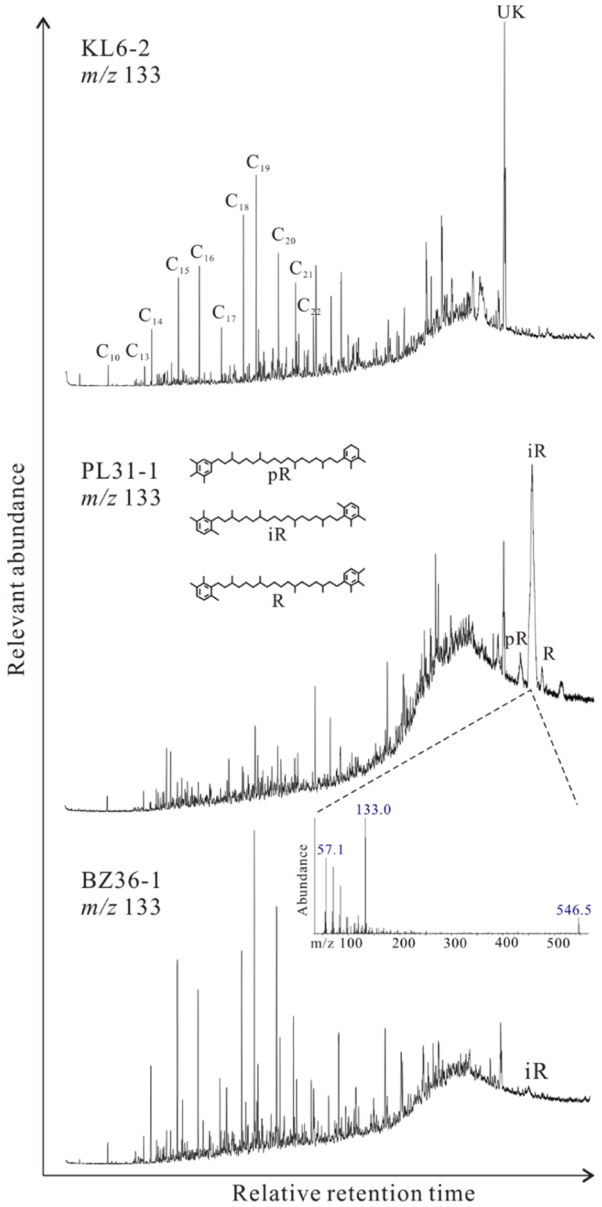


**Figure 9.** Representative *m/z* 133 mass chromatograms, showing the distributions of monoaryl isoprenoids ($C_{10}$–$C_{22}$), paleorenieratane, isorenieratane, and renieratane (R) which are typical biomarkers for green sulfur bacteria (*Chlorobiaceae*). UK: unknown compound.

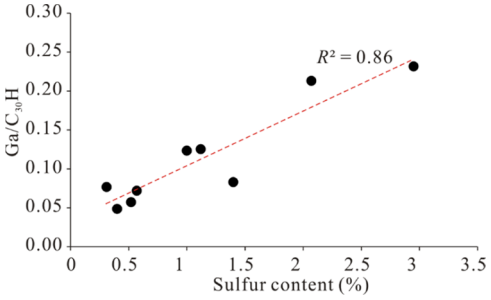


**Figure 10.** Cross-plot of the sulfur content vs Ga/$C_{30}$H, indicating the positive influence of a reducing environment on the sulfur content.

reasons for the presence of low concentrated isorenieratane are tentatively explained. First, the effects of migration might result in the loss of some micromolecular biomarkers including isorenieratane. Second, isorenieratane might be degraded when the corresponding source rocks experience the diagenesis process. Third, the high primary productivity at the upper chemocline might influence the wavelength distribution of light. Thus, the relative distribution of green sulfur bacteria might be influenced. Clearly, the occurrence of brown-pigmented green sulfur bacteria means a reducing water column. Together with the HSOs and abundance of organic sulfur compounds, indicating the good preservation of organic matters. Moreover, the ratio of pristane (Pr) to phytane (Ph) is quite low (0.85−1.17) among the HSOs in a reducing sedimentary environment.[132] It is worth nothing that isorenieratane is also identified in the LSOs and the Pr/Ph ratio is in the range of 1.1−1.3, implying that the paleo-water column is also under a reducing condition. However, no sulfide hopanes in biomarkers are identified in LSOs. The BSR reaction might probably also occur at the corresponding reducing water column. Nevertheless, hydrogen sulfide may be preferentially consumed by abundant ferric ions in sediments to produce early diagenetic pyrite, resulting in a low sulfur content of organic matter.[133]

The isotopically depleted $^{13}C$ isotope values of aromatic secohopanes in all samples indicate the occurrence of a methane cycle during the depositional period, suggesting that methane is used by special microbes as the main carbon source and energy.[122,134] Volkman et al.[18] reported that $C_{29}$ neohop-13(18)-ene and $C_{30}$ hop-17(21)-ene had very negative $^{13}C$ isotope values (−50.8 and −43.7‰, respectively) in the Huadian shale under reducing depositional conditions. This is attributed to the depletion of $^{13}C$ isotope values to the contribution of methanotrophs even though 3$\beta$-methylhopanes and other biomarkers indicative for the methanotrophic bacterial activity were not detected. Similarly, Xie et al.[135] found that stable carbon isotopes of $C_{29}$ and $C_{30}$ 17$\alpha$, 21$\beta$(H)-hopanes had a range of −45.6 to −61.5‰ in the Lucaogou formation oil shale from the Junggar Basin, considerably lighter than the *n*-alkanes (ca. −34‰), suggesting the contribution of methanotrophs. The $^{13}C$ isotope values of $C_{29}$ secohopanes (−45.6−41.2‰) and $C_{30}$ secohopanes (−45−42.3‰) are very similar to the isotopes' depleted values of hopanes in sediments in which methanotrophs use methane as a carbon source.[105] Methane is produced by methanogenic archaea, which are anaerobic bacteria,[136] while free-living aerobic methanotrophs are often concentrated at the microaerophilic interface between oxic and anoxic zones (chemocline).[137] Probably, the water column stratification might lead to the coexistence of anaerobic bacteria (methanogenic and sulfur-reducing bacteria) and aerobic bacteria (methanotrophs). The gammacerane index of HSOs is in the range of 0.12−0.23, suggesting the stratification of a water column and possibly the brackish water conditions.

**5.4. Geological Implications of Hopanoids.** Besides the regular parameters of hopanes, secohopanes, aromatic 8,14-secohopanes, and sulfide hopanes have also been altered during the diagenetic process.[84,102]

In our samples, the MAH parameters also have good correlations ($R^2$ = 0.67 and 0.62, respectively) with maturity parameters of saturated hydrocarbons including Ts/(Ts + Tm) and $C_{29}$ $\beta\beta/(\alpha\alpha + \beta\beta)$, although the MAH parameter is in a narrow range of 0.83−0.94 (Figure 11). The ratio of moretane/hopane is the typical parameter to indicate the maturity of samples because of the transformation of $\beta\alpha$-


https://doi.org/10.1021/acsomega.1c02762
ACS Omega 2021, 6, 30298−30314

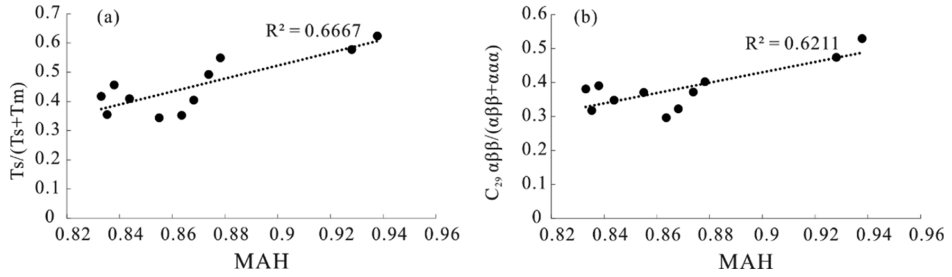


**Figure 11.** Correlations of MAH vs Ts/(Ts + Tm) (a) and $C_{29}$ $\alpha\beta\beta/(\alpha\alpha\alpha + \alpha\beta\beta)$ (b), showing good correlations between two parameters.

moretane to $\alpha\beta$-hopane under thermal effects.[106] However, only some studies reported the application of 8,14-secohopanes in saturated hydrocarbons.[82,119] The ratios of $C_{31}$−$C_{35}$ secomoretanes/secohopanes all have good negative correlations with maturity parameters including Ts/(Ts + Tm), $C_{29}$ $\beta\beta/(\alpha\alpha + \beta\beta)$, and $C_{29}$ 20S/(20S + 20R) (Figure 7), suggesting that the distributions of secomoretanes and secohopanes are also influenced by mature effects in the studied samples in this region. The complexity of these compounds might indicate that the distributions are controlled by comprehensive factors. At least, the thermal effect might influence the evolution of 8,14-secohopanes in saturated hydrocarbons.

Aromatic 8,14-secohopanes were thought to be formed via thermal degradation of hopanes.[87,101] The sequence of formation is SHs to DSHs to IDs.[87] In contrast, IDs are more enriched in lower-maturity samples, while DSHs are enriched in higher-maturity samples (Figure 8). This suggests that other reactions might have participated in the formation of aromatic 8,14-secohopanes except thermal maturity.

Besides the thermal effects on the distribution mode of hopanoids, the depositional environments also greatly impact the formation of hopanoids,[106] especially the sulfide hopanes. The decreasing relative abundance from $C_{30}$ hopane to $C_{35}$ hopane is normal in oil samples. However, the relative abundance of $C_{35}$ hopane in HSOs is higher than in LSOs, even slightly higher than the $C_{34}$ hopane in HSOs, suggesting a reducing depositional environment. However, the relative abundance of sulfide hopane is completely different from the distribution of hopanes (Figure 12). The preferential incorporation of inorganic sulfur into bacteriohopanepolyol derivates leading to preservation of the intact carbon skeleton[14,37] might result in the dominance of $C_{35}$ sulfide hopane (Figure 12). The ratio of $C_{35}/C_{34}$ sulfide hopane is in the range of 2.4−2.9, obviously higher than $C_{35}/C_{34}$ hopane (0.82−1.00), suggesting that the incorporation of sulfur might protect the original carbon skeleton of bacteriohopanepolyol. The co-elution of compound B and $C_{32}$SH-1 results in the high abundance of $C_{32}$ sulfide hopane (Figure 5). The ratio of $C_{35}/C_{34}$ sulfide hopane has a good correlation with $C_{35}S/C_{34}S$ (Figure 13a), indicating that the long side-chain sulfide hopanes also experience a similar diagenesis evolution of hopanes in the low-mature to mature stage. Similarly, $C_{35}$SH-2/$C_{35}$SH-1 with the range of 0.90−1.56 has good correlations ($R^2$ = 0.99 and 0.88, respectively) with $C_{35}S/C_{34}S$ and Ga/$C_{30}$H (Figure 13b,c), indicating that this ratio could be influenced by the reducing depositional environment. The sulfide hopanes are formed under the sulfur-containing bottom water column. The redox water environment might influence the distributions of compounds. Because of the low-mature to mature stage of the samples, the $C_{35}$SH-2/$C_{35}$SH-1 ratio is

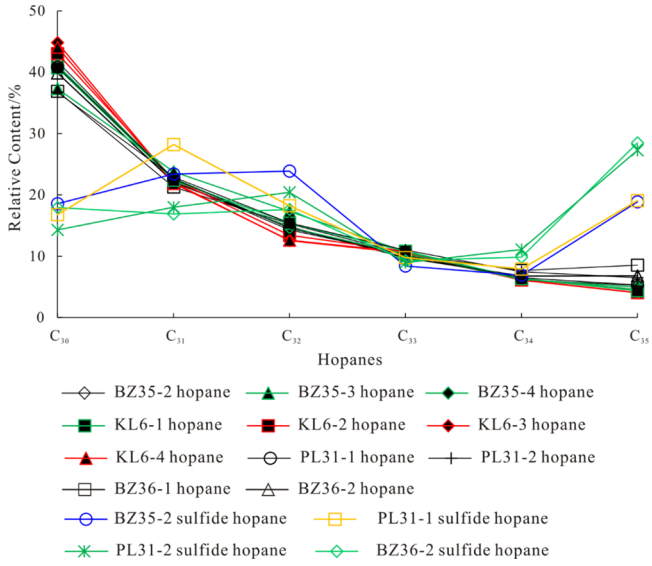


**Figure 12.** Relative distribution of $C_{30}$−$C_{35}$ hopanes and sulfide hopanes.

mainly affected by the reducing depositional environment. In addition, the ratio of $C_{35}/C_{34}$ benzohopane in the range of 0.30−0.94 also has a good correlation ($R^2$ = 0.79) with that of the $C_{35}S/C_{34}S$ hopane (Figure 13d). It is proposed that the long side-chain hopanoids in a reducing depositional environment may have experienced a similar evolution process, leading to good correlation between $C_{35}$ and $C_{34}$ hopanoids, although the hopanoids have different molecular structures.

Hopanoids are abundant in sediments and crude oils, and the compounds are very resistant to biodegradation.[4,5,7] The parameters of hopanes can be used as an oil−source correlation, for maturity evaluation, and for depositional environment analyses, such as $C_{31}$22R/$C_{30}$H, Ts/(Ts + Tm), $C_{29}$Ts/($C_{29}$H + $C_{29}$Ts), $C_{35}S/C_{34}S$, $C_{31}/C_{30}$H, $C_{29}/C_{30}$H, $C_{31}$−$C_{35}$ 22S/(22S + 22R), and others.[106] In addition, the secohopanes, aromatic 8,14-secohopanes, and sulfide hopanes are influenced by the thermal effects and depositional conditions of related source rocks. These compounds can provide more detailed information for the formation of high-sulfur crude oils. This knowledge provides a refined possibility of oil−oil and oil−source correlations. The BSR-derived high-sulfur crude oils were sourced from the source rocks under reducing paleo-conditions with water column stratification. This organic sedimentary environment is in favor of the growth of diverse microorganisms and preservation of the organic matter during the diagenetic process, resulting in the influence of some ratios, including $C_{35}/C_{34}$ sulfide hopane, $C_{35}$SH-2/$C_{35}$SH-1, and $C_{35}/C_{34}$ benzohopane. The parameter of $C_{31}$−


https://doi.org/10.1021/acsomega.1c02762
ACS Omega 2021, 6, 30298−30314

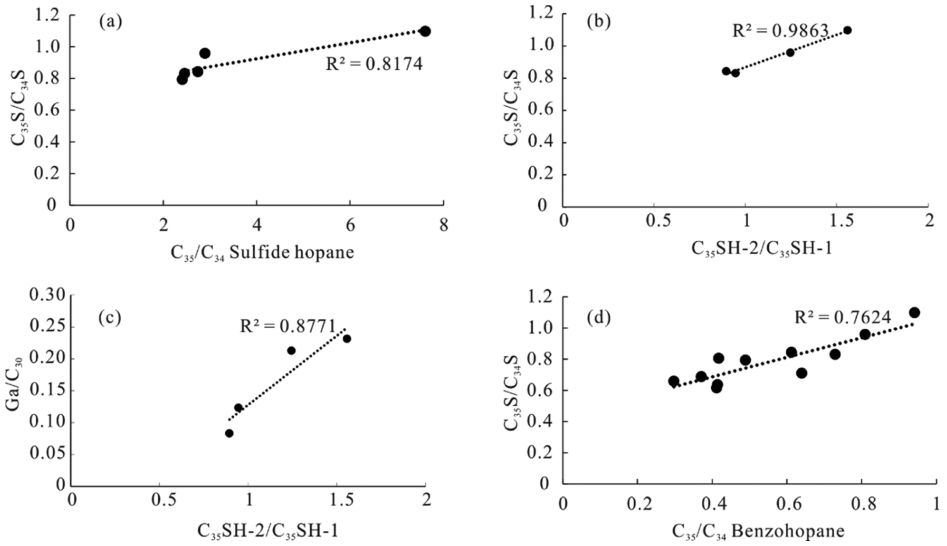


**Figure 13.** Cross-plots of $C_{35}/C_{34}$ sulfide hopane vs $C_{35}S/C_{34}S$ (a); $C_{35}$SH-2/$C_{35}$SH-1 vs $C_{35}S/C_{34}S$ (b) and Ga/$C_{30}$H (c); and $C_{35}/C_{34}$ benzohopane $C_{35}S/C_{34}S$ (d). $C_{35}S/C_{34}S$: $C_{35}$ 22S, 17$\alpha$(H), 21$\beta$(H)-hopane/$C_{34}$ 22S, 17$\alpha$(H), 21$\beta$(H)-hopane; $C_{35}$SH-2/$C_{35}$SH-1: compound-2/compound-1 of $C_{35}$ sulfide hopane.

$C_{35}$ secomoretanes/secohopanes is tentatively affected by the thermal effect in samples in the region.

## 6. CONCLUSIONS

Abundant hopanoids are identified in oils, including hopanes, secohopanes, 25-norhopanes, benzohopanes, aromatized secohopanes, and sulfide hopanes. The very depleted $^{13}C$ isotope values of $C_{29}$ and $C_{30}$ D-ring-monoaromatic-8,14-secohopanes indicate the presence of methane-oxidating bacteria (methanotrophs). The bacteria sulfate reduction results in the formation of HSOs. Perhaps, the stratification of the paleowater column results in diverse microorganisms living in the oxic and anoxic environments.

The thermal effects and depositional environments influence the distributions of the parameters of secohopanes, aromatic 8,14-secohopanes, and sulfide hopanes. The ratios of $C_{31}$−$C_{35}$ secomoretanes/secohopanes are mainly controlled by the maturity in the low-mature to mature stage in the studied samples in this region, showing the good negative correlations between $C_{31}$−$C_{35}$ secomoretanes/secohopanes and maturity parameters of the saturates. Long side-chain hopanoids in a reducing depositional environment may experience a similar evolution process in the low-mature to mature stage, resulting in good correlations between $C_{35}/C_{34}$ sulfide hopane, compound-2/compound-1 $C_{35}$ sulfide hopane, $C_{35}/C_{34}$ benzohopanes, and $C_{35}S/C_{34}S$ hopanes and the gammacerane index. The hopanoids in the saturates, aromatics, and sulfide fractions provide comprehensive information for high-sulfur crude oils, which is suitable for further oil−source rock correlations and exploration of HSOs in the Huanghekou Eastern Sag and the Laizhouwan Northeastern Sag..

## ■ ASSOCIATED CONTENT

### Supporting Information

The Supporting Information is available free of charge at https://pubs.acs.org/doi/10.1021/acsomega.1c02762.

Mass spectra of $C_{29}$ 8,14-secohopanes, $C_{30}$ 8,14-secohopanes, $C_{32}$ benzohopane, $C_{33}$ benzohopane, $C_{34}$ benzohopane, $C_{35}$ benzohopane, $C_{29}$ D-ring monoaromatic 8,14-secohopanoid, $C_{30}$ D-ring monoaromatic 8,14-secohopanoid, $C_{28}$ D-ring monoaromatic 8,14-seco-28-nor-hopanoid, $C_{29}$ D-ring monoaromatic 8,14-seco-28-nor-hopanoid, $C_{29}$ indenyldrimane, $C_{30}$ indenyldrimane, Compound-1 of $C_{31}$ sulfide hopane, Compound-2 of $C_{31}$ sulfide hopane, peak at Compound-1 of $C_{32}$ sulfide hopane, and Compound-2 of $C_{32}$ sulfide hopane (PDF)

## ■ AUTHOR INFORMATION


### Corresponding Author

**Dujie Hou** − *School of Energy Resources and Key Laboratory of Marine Reservoir Evolution and Hydrocarbon Accumulation Mechanism, Ministry of Education, China University of Geosciences (Beijing), Beijing 100083, China;* orcid.org/0000-0003-2001-4082; Email: houdj313@163.com

### Authors

**Congkai Niu** − *School of Energy Resources and Key Laboratory of Marine Reservoir Evolution and Hydrocarbon Accumulation Mechanism, Ministry of Education, China University of Geosciences (Beijing), Beijing 100083, China*

**Xiong Cheng** − *School of Energy Resources and Key Laboratory of Marine Reservoir Evolution and Hydrocarbon Accumulation Mechanism, Ministry of Education, China University of Geosciences (Beijing), Beijing 100083, China;* orcid.org/0000-0002-2991-1137

**Xu Han** − *School of Energy Resources and Key Laboratory of Marine Reservoir Evolution and Hydrocarbon Accumulation Mechanism, Ministry of Education, China University of Geosciences (Beijing), Beijing 100083, China*

**Yan Li** − *School of Energy Resources and Key Laboratory of Marine Reservoir Evolution and Hydrocarbon Accumulation Mechanism, Ministry of Education, China University of Geosciences (Beijing), Beijing 100083, China*

**Yaxi Li** − *Consulting and Research Center, Ministry of Natural Resources, Beijing 100035, China*

Complete contact information is available at: https://pubs.acs.org/10.1021/acsomega.1c02762




https://doi.org/10.1021/acsomega.1c02762
*ACS Omega* 2021, 6, 30298−30314

### Notes

The authors declare no competing financial interest.

## ■ ACKNOWLEDGMENTS

This research was supported by the National Natural Science Foundation of China (grant no. 41872131). The authors are highly indebted to the associate editor Mohamed Mahmoud and anonymous reviewers for thorough and constructive reviews that greatly improved the clarity and quality of this article. They would like to express their thanks to Dr. Wenjing Ding and Dr. Huiyuan Xu for modifying the English writing.

## ■ REFERENCES

(1) Ourisson, G.; Rohmer, M.; Poralla, K. Prokaryotic hopanoids and other polyterpenoid sterol surrogates. *Annu. Rev. Microbiol.* **1987**, *41*, 301−333.
(2) Rohmer, M.; Bisseret, P.; Neunlist, S. The hopanoids, prokaryotic triterpenoids and precursors of ubiquitous molecular fossils. In *Biological Markers in Sediments and Petroleum*; Moldowan, J. M., Albrecht, P., Philp, R. P., Eds.; Prentice Hall: Englewood Cliffs, New Jersey, 1992; pp 1−17.
(3) Zhu, C.; Cui, X.; He, Y.; Kong, L.; Sun, Y. Extended 3$\beta$-methylhopanes up to C45 in source rocks from the Upper Cretaceous Qingshankou Formation, Songliao Basin, northeast China. *Org. Geochem.* **2020**, *142*, 103998.
(4) Head, I. M.; Jones, D. M.; Larter, S. R. Biological activity in the deep subsurface and the origin of heavy oil. *Nature* **2003**, *426*, 344−352.
(5) Larter, S.; Huang, H.; Adams, J.; Bennett, B.; Snowdon, L. R. A practical biodegradation scale for use in reservoir geochemical studies of biodegraded oils. *Org. Geochem.* **2012**, *45*, 66−76.
(6) Peters, K. E.; Moldowan, J. M. *The Biomarker Guide. Interpreting Molecular Fossils in Petroleum and Ancient Sediments*; Prentice Hall: Englewood Cliffs, 1993.
(7) Wenger, L. M.; Davis, C. L.; Isaksen, G. H. Multiple controls on petroleum biodegradation and impact on oil quality. *SPE Reservoir Eval. Eng.* **2002**, *5*, 375−383.
(8) Wang, Z.; Fingas, M.; Page, D. S. Oil spill identification. *J. Chromatogr. A* **1999**, *843*, 369−411.
(9) Wang, Z.; Stout, S. A.; Fingas, M. Forensic fingerprinting of biomarkers for oil spill characterization and source identification. *Environ. Forensics* **2006**, *7*, 105−146.
(10) John, G. F.; Han, Y.; Clement, T. P. Fate of hopane biomarkers during in-situ burning of crude oil - A laboratory-scale study. *Mar. Pollut. Bull.* **2018**, *133*, 756−761.
(11) Han, Y.; John, G. F.; Clement, T. P. Understanding the thermal degradation patterns of hopane biomarker compounds present in crude oil. *Sci. Total Environ.* **2019**, *667*, 729−798.
(12) Greiner, A. C.; Spyckerelle, C.; Albrecht, P.; Ourisson, G. Aromatic hydrocarbons from geological sources. Part V. Mono- and di-aromatic hopane derivatives. *J. Chem. Res.* **1977**, *334*, 3829−3871.
(13) Peters, K. E.; Moldowan, J. M. Effects of source, thermal maturity, and biodegradation on the distribution and isomerization of homohopanes in petroleum. *Org. Geochem.* **1991**, *17*, 47−61.
(14) Sinninghe Damsté, J. S.; van Duin, A. C. T.; Hollander, D.; Kohnen, M. E. L.; de Leeuw, J. W. Early diagenesis of bacteriohopanepolyol derivatives: Formation of fossil homohopanoids. *Geochim. Cosmochim. Acta* **1995**, *59*, 5141−5157.
(15) Moldowan, J. M.; McCaffrey, M. A. A novel microbial hydrocarbon degradation pathway revealed by hopane demethylation in a petroleum reservoir. *Geochim. Cosmochim. Acta* **1995**, *59*, 1891−1894.
(16) van Winden, J. F.; Talbot, H. M.; Kip, N.; Reichart, G.-J.; Pol, A.; McNamara, N. P.; Jetten, M. S. M.; op den Camp, H. J. M.; Sinninghe Damsté, J. S. Bacteriohopanepolyol signatures as markers for methanotrophic bacteria in peat moss. *Geochim. Cosmochim. Acta* **2012**, *77*, 52−61.
(17) Eickhoff, M.; Birgel, D.; Talbot, H. M.; Peckmann, J.; Kappler, A. Diagenetic degradation products of bacteriohopanepolyols produced by Rhodopseudomonas palustris strain TIE-1. *Org. Geochem.* **2014**, *68*, 31−38.
(18) Volkman, J. K.; Zhang, Z. R.; Xie, X. M.; Qin, J. Z.; Borjigin, T. Biomarker evidence for *Botryococcus* and a methane cycle in the Eocene Huadian oil shale, NE China. *Org. Geochemistry* **2015**, *78*, 121−134.
(19) Rohmer, M. The biosynthesis of the triterpenoids of the hopane series in the Eubacteria: a mine of new enzyme reactions. *Pure Appl. Chem.* **1993**, *65*, 1293−1298.
(20) Zhao, N.; Berova, N.; Nakanishi, K.; Rohmer, M.; Mougenot, P.; Jürgens, U. J. Structures of two bacteriohopanoids with acyclic pentol side-chains from the cyanobacterium *Nostoc* PCC 6720. *Tetrahedron* **1996**, *52*, 2777−2788.
(21) Summons, R. E.; Jahnke, L. L.; Hope, J. M.; Logan, G. A. 2-Methylhopanoids as biomarkers for cyanobacterial oxygenic photosynthesis. *Nature* **1999**, *400*, 554−557.
(22) Talbot, H. M.; Watson, D. F.; Murrell, J. C.; Carter, J. F.; Farrimond, P. Analysis of intact bacteriohopanepolyols from methanotrophic bacteria by reversed-phase high-performance liquid chromatography-atmospheric pressure chemical ionisation mass spectrometry. *J. Chromatogr. A* **2001**, *921*, 175−185.
(23) Talbot, H. M.; Farrimond, P. Bacterial populations recorded in diverse sedimentary biohopanoid distributions. *Org. Geochem.* **2007**, *38*, 1212−1225.
(24) Meredith, W.; Snape, C. E.; Carr, A. D.; Nytoft, H. P.; Love, G. D.; Love, G. D. The occurrence of unusual hopenes in hydropyrolysates generated from severely biodegraded oil seep asphaltenes. *Org. Geochem.* **2008**, *39*, 1243−1248.
(25) Sinninghe Damsté, J. S.; Schouten, S.; Volkman, J. K. C27-C30 neohop-13(18)-enes and their saturated and aromatic derivatives in sediments: Indicators for diagenesis and water column stratification. *Geochim. Cosmochim. Acta* **2014**, *133*, 402−421.
(26) Nytoft, H. P. Novel side chain methylated and hexacyclic hopanes: Identification by synthesis, distribution in a worldwide set of coals and crude oils and use as markers for oxic depositional environments. *Org. Geochem.* **2011**, *42*, 520−539.
(27) Nytoft, H. P.; Ingermann Petersen, H.; Bryld Wessel Fyhn, M.; Nielsen, L. H.; Hovikoski, J.; Abatzis, I. Novel saturated hexacyclic C34 and C35 hopanes in lacustrine oils and source rocks. *Org. Geochem.* **2015**, *87*, 107−118.
(28) Moldowan, J. M.; Fago, F. J.; Carlson, R. M. K.; Young, D. C.; an Duvne, G.; Clardy, J.; Schoell, M.; Pillinger, C. T.; Watt, D. S. Rearranged hopanes in sediments and petroleum. *Geochem. Cosmochim. Acta* **1991**, *55*, 3333−3353.
(29) Jiang, L.; George, S. C.; Zhang, M. The occurrence and distribution of rearranged hopanes in crude oils from the Lishu Depression, Songliao Basin, China. *Org. Geochem.* **2018**, *115*, 205−219.
(30) Wang, X.; Zhao, W.; Zhang, S.; Wang, H.; Su, J.; Canfield, D. E.; Hammarlund, E. U. The aerobic diagenesis of Mesoproterozoic organic matter. *Sci. Rep.* **2018**, *8*, 13324.
(31) Jin, X.; Zhang, Z.; Wu, J.; Zhang, C.; He, Y.; Cao, L.; Zheng, R.; Meng, W.; Xia, H. Origin and geochemical implication of relatively high abundance of 17$\alpha$ (H)-diahopane in Yabulai basin, northwest China. *Mar. Pet. Geol.* **2019**, *99*, 429−442.
(32) Xiao, H.; Li, M.; Wang, T.; You, B.; Leng, J.; Han, Q.; Ran, Z.; Wang, X.; Gao, Z. Four series of rearranged hopanes in the Mesoproterozoic sediments. *Chem. Geol.* **2021**, *573*, 120210.
(33) Liao, J.; Lu, H.; Sheng, G.; Peng, P. A.; Hsu, C. S. Monoaromatic, Diaromatic, Triaromatic, and Tetraaromatic Hopanes in Kukersite Shale and Their Stable Carbon Isotopic Composition. *Energy Fuels* **2015**, *29*, 3573−3583.
(34) Rybicki, M.; Marynowski, L.; Simoneit, B. R. T. Benzohopane Series, Their Novel Di-, Tri-, and Tetraaromatic Derivatives, and Diaromatic 23- and 24-Norbenzohopanes from the Lower Jurassic Blanowice Formation, Southern Poland. *Energy & Fules* **2017**, *31*, 2617−2624.


https://doi.org/10.1021/acsomega.1c02762
*ACS Omega* 2021, 6, 30298−30314

(35) Valisolalao, J.; Perakis, N.; Chappe, B.; Albrecht, P. A novel sulfur containing C35 hopanoid in sediments. *Tetrahedron Lett.* **1984**, *25*, 1183−1186.
(36) Cyr, T. D.; Payzant, J. D.; Montgomery, D. S.; Strausz, O. P. A homologous series of novel hopane sulfides in petroleum. *Org. Geochem.* **1986**, *9*, 139−143.
(37) Schaeffer, P.; Adam, P.; Philippe, E.; Trendel, J. M.; Schmid, J.-C.; Behrens, A.; Connan, J.; Albrecht, P. The wide diversity of hopanoid sulfides evidenced by the structural identification of several novel hopanoid series. *Org. Geochem.* **2006**, *37*, 1590−1616.
(38) Sinninghe Damste, J. S.; Rijpstra, W. I. C.; Kock-van Dalen, A. C.; de Leeuw, J. W.; Schenck, P. A. Quenching of labile functionalized lipids by inorganic sulphur species. Evidence for the formation of sedimentary organic sulphur compounds at the early stages of diagenesis. *Geochim. Cosmochim. Acta* **1989**, *53*, 1343−1355.
(39) Adam, P.; Schmid, J. C.; Mycke, B.; Strazielle, C.; Connan, J.; Huc, A.; Riva, A.; Albrecht, P. Structural investigation of nonpolar sulfur cross-linked macromolecules in petroleum. *Geochim. Cosmochim. Acta* **1993**, *57*, 3395−3419.
(40) Adam, P.; Schneckenburger, P.; Schaeffer, P.; Albrecht, P. Clues to early diagenetic sulfurization processes from mild chemical cleavage of labile sulfur-rich geomacromolecules. *Geochim. Cosmochim. Acta* **2000**, *64*, 3485−3503.
(41) Oldenburg, T. B. P.; Huang, H.; Donohoe, P.; Willsch, H.; Larter, S. R. High molecular weight aromatic nitrogen and other novel hopanoid-related compounds in crude oils. *Org. Geochem.* **2004**, *35*, 665−678.
(42) Adam, P.; Schaeffer, P.; Schmitt, G.; Bailly, L.; Courel, B.; Fresnais, M.; Fossurier, C.; Rohmer, M. Identification and mode of formation of hopanoid nitriles in archaeological soils. *Org. Geochem.* **2016**, *91*, 100−108.
(43) Sinninghe Damsté, J. S.; Rijpstra, W. I. C.; Schouten, S.; Fuerst, J. A.; Jetten, M. S. M.; Strous, M. The occurrence of hopanoids in planctomycetes: Implications for the sedimentary biomarker record. *Org. Geochem.* **2004**, *35*, 561−566.
(44) Shatz, M.; Yosief, T.; Kashman, Y. Bacteriohopanehexol, a new triterpene from the marine sponge *Petrosia* species. *J. Nat. Prod.* **2000**, *63*, 1554−1556.
(45) Blumenberg, M.; Hoppert, M.; Krüger, M.; Dreier, A.; Thiel, V. Novel findings on hopanoid occurrences among sulfate reducing bacteria: Is there a direct link to nitrogen fixation? *Org. Geochem.* **2012**, *49*, 1−5.
(46) Lodha, T. D.; Srinivas, A.; Sasikala, C.; Ramana, C. V. Hopanoid inventory of *Rhodoplanes spp*. *Arch. Microbiol.* **2015**, *197*, 861−867.
(47) Grice, K.; Audino, M.; Boreham, C. J.; Alexander, R.; Kagi, R. I. Distributions and stable carbon isotopic compositions of biomarkers in torbanites from different palaeogeographical locations. *Org. Geochem.* **2001**, *32*, 1195−1210.
(48) Zhang, Y.; Sun, Y.; Chen, J. Stable carbon isotope evidence for the origin of C28 steranes in lacustrine source rocks from the Qikou Sag, Bohai Bay Basin, Eastern China. *Org. Geochem.* **2020**, *145*, 104028.
(49) Xu, H.; George, S. C.; Hou, D.; Cao, B.; Chen, X. Petroleum sources in the Xihu Depression, East China Sea: Evidence from stable carbon isotopic compositions of individual n-alkanes and isoprenoids. *J. Pet. Sci. Eng.* **2020**, *190*, 107073.
(50) Freeman, K. H.; Hayes, J. M.; Trendel, J.-M.; Albrecht, P. Evidence from carbon isotope measurements for diverse origins of sedimentary hydrocarbons. *Nature* **1990**, *343*, 254−256.
(51) Hayes, J. M.; Freeman, K. H.; Popp, B. N.; Hoham, C. H. Compound-specific isotopic analyses: a novel tool for reconstruction of ancient biogeochemical processes. *Org. Geochem.* **1990**, *16*, 1115−1128.
(52) Dawson, D.; Grice, K.; Alexander, R.; Edwards, D. The effect of source and maturity on the stable isotopic compositions of individual hydrocarbons in sediments and crude oils from the Vulcan Sub-basin, Timor Sea, Northern Australia. *Org. Geochem.* **2007**, *38*, 1015−1038.
(53) Li, Y.; Song, Z.; Cao, X.-x.; George, S. C. Sedimentary organic matter record of Early Cretaceous environmental changes in western Liaoning Province, NE China. *Org. Geochem.* **2016**, *98*, 54−65.
(54) Schwarzbauer, J.; Littke, R.; Meier, R.; Strauss, H. Stable carbon isotope ratios of aliphatic biomarkers in Late Palaeozoic coals. *Int. J. Coal Geol.* **2013**, *107*, 127−140.
(55) Shawar, L.; Said-Ahmad, W.; Ellis, G. S.; Amrani, A. Sulfur isotope composition of individual compounds in immature organic-rich rocks and possible geochemical implications. *Geochim. Cosmochim. Acta* **2020**, *274*, 20−44.
(56) Shawar, L.; Grice, K.; Holman, A. I.; Amrani, A. Carbon and sulfur isotopic composition of alkyl- and benzo-thiophenes provides insights into their origins and formation pathways. *Org. Geochem.* **2021**, *151*, 104163.
(57) Jiang, P.; Yang, B.; Zheng, Z.; Lai, W.; Yang, X. Characteristics on reservoir forming of Tertiary in Bohai Sea area. *Pet. Geol. Recovery Effic.* **2003**, *10*, 16−19. (in Chinese with English abstract)
(58) Jiang, F.; Pang, X.; Bai, J.; Zhou, X.; Li, J.; Guo, Y. Comprehensive assessment of source rocks in the Bohai Sea area, eastern China. *AAPG Bull.* **2016**, *100*, 969−1002.
(59) Allen, M. B.; Macdonald, D. I. M.; Xun, Z.; Vincent, S. J.; Brouet-Menzies, C. Early Cenozoic two-phase extension and late Cenozoic thermal subsidence and inversion of the Bohai Basin, northern China. *Mar. Pet. Geol.* **1997**, *14*, 951−972.
(60) Guo, X.; Liu, K.; He, S.; Song, G.; Wang, Y.; Hao, X.; Wang, B. Petroleum generation and charge history of the northern Dongying Depression, Bohai Bay Basin, China: insight from integrated fluid inclusion analysis and basin modelling. *Mar. Pet. Geol.* **2012**, *32*, 21−35.
(61) Yang, Y.; Xu, T. Hydrocarbon habitat of the offshore Bohai Basin, China. *Mar. Pet. Geol.* **2004**, *21*, 691−708.
(62) Ye, M.; Xie, X.; Xu, C.; Du, X.; Du, X.; Song, Z. Sedimentary features and their controls in a mixed siliciclastic-carbonate system in a shallow lake area: An example from the BZ-X block in the Huanghekou Sag, Bohai Bay Basin, Eastern China. *Geol. J.* **2018**, *54*, 2016−2033.
(63) Jiu, K.; Ding, W.; Huang, W.; Zhang, Y.; Zhao, S.; Hu, L. Fractures of lacustrine shale reservoirs, the Zhanhua Depression in the Bohai Bay Basin, eastern China. *Mar. Pet. Geol.* **2013**, *48*, 113−123.
(64) Xia, Y.; Zhang, G. Investigation of mechanisms of formation of biphenyls and benzonaphthothiophenes by simulation experiment. *Sci. China* **2002**, *45*, 392−398.
(65) Wu, L.; Xu, H.; Cheng, J. Evolution of sedimentary system and analysis of sedimentary source in Paleogene of Bozhong sag, Bohai Bay. *Mar. Geol. Quat. Geol.* **2006**, *26*, 81−88. (in Chinese with English abstract)
(66) Wang, F. L.; Tang, G. M.; Chen, R. T.; Wang, G. Y.; Yu, Q. Thickening mechanism and reservoir formation model of Bozhong 29-6 Oilfield in Huanghekou sag, Bohai Bay Basin. *Earth Sci.* **2020**. (in Chinese with English abstract).
(67) Wu, K. Q.; Jiang, X.; Sun, H. F. Model of lacustrine source rocks in offshore oil kitchen sags: A case study of Paleogene in Huanghekou Sag. *Geol. Sci. Technol. Inf.* **2015**, *34*, 64−70.
(68) Yang, H.; Wang, D.; Gao, Y.; Wang, J.; Li, Z.; Qian, G. Neogene natural gas genesis and hydrocarbon differential enrichment mechanism in the basin marginal sag of Bohai Bay Basin: a case study of the eastern subsag of Huanghekou sag. *Acta Pet. Sin.* **2019**, *40*, 509−518. (in Chinese with English abstract)
(69) Xu, T.; Hou, D.; Zhao, Z.; Wang, Y.; Xu, C.; Wang, F. Controlling factors for the development of high-quality source rocks in Huanghekou East Sag of Bohai Bay Basin. *J. Northeast Pet. Univ.* **2017**, *41*, 11−20. (in Chinese with English abstract)
(70) Peng, W.; Xin, R.; Sun, H.; Wu, K.; Shi, H.; Wang, D. Formation and evolution of Laizhou Bay sag in Bohai Bay. *Acta Pet. Sin.* **2009**, *30*, 654−660. (in Chinese with English abstract)
(71) Zhao, Z.; Hou, D.; Cheng, X.; Xu, H.; Ma, C.; Zhou, X.; Xu, C. Geochemical and palynological characteristics of the Paleogene source rocks in the Northeastern Laizhouwan Sag, Bohai Bay Basin, China: Hydrocarbon potential, depositional environment, and factors


https://doi.org/10.1021/acsomega.1c02762
*ACS Omega* 2021, 6, 30298−30314

controlling organic matter enrichment. *Mar. Pet. Geol.* **2021**, *124*, 104792.
(72) Niu, C. K.; Hou, D. J.; Cheng, X.; Han, X.; Li, Y. X. Organic geochemical characteristics of crude oils in Bohai Bay marginal sags: implications for the distribution of dibenzothiophenes. *Mar. Petrol. Geol.* Under Review.
(73) Brocks, J. J.; Schaeffer, P. Okenane, a biomarker for purple sulfur bacteria (Chromatiaceae), and other new carotenoid derivatives from the 1640Ma Barney Creek Formation. *Geochim. Cosmochim. Acta* **2008**, *72*, 1396−1414.
(74) Cheng, X.; Hou, D.; Xu, C.; Wang, F. Biodegradation of tricyclic terpanes in crude oils from the Bohai Bay Basin. *Org. Geochem.* **2016**, *101*, 11−21.
(75) Jiang, A.; Zhou, P.; Sun, Y.; Xie, L. Rapid column chromatography separation of alkylnaphthalenes from aromatic components in sedimentary organic matter for compound specific stable isotope analysis. *Org. Geochem.* **2013**, *60*, 1−8.
(76) Wang, M.; Zhao, S.; Chung, K. H.; Xu, C.; Shi, Q. Approach for Selective Separation of Thiophenic and Sulfidic Sulfur Compounds from Petroleum by Methylation/Demethylation. *Anal. Chem.* **2015**, *87*, 1083−1088.
(77) Wu, J.; Zhang, W.; Ma, C.; Wang, F.; Zhou, X.; Chung, K. H.; Hou, D.; Zhang, Y.; Shi, Q. Isolation and characterization of sulfur compounds in a lacustrine crude oil. *Fuel* **2019**, *253*, 1482−1489.
(78) Ourisson, G.; Albrecht, P.; Rohmer, M. The hopanoids: palaeochemistry and biochemistry of a group of natural products. *Pure Appl. Chem.* **1979**, *51*, 709−729.
(79) Ourisson, G.; Albrecht, P. Hopanoids. 1. Geohopanoids: the most abundant natural products on Earth? *Acc. Chem. Res.* **1992**, *25*, 398−402.
(80) Connan, J.; Bouroullec, J.; Dessort, D.; Albrecht, P. The microbial input in carbonate-anhydrite facies of a sabkha palaeoenvironment from Guatemala: A molecular approach. *Org. Geochem.* **1986**, *10*, 29−50.
(81) Volkman, J. K.; Alexander, R.; Kagi, R. I.; Woodhouse, G. W. Demethylated hopanes in crude oils and their applications in petroleum geochemistry. *Geochim. Cosmochim. Acta* **1983**, *47*, 785−794.
(82) Villar, H. J.; Püttmann, W. Geochemical characteristics of crude oils from the Cuyo Basin, Argentina. *Argentina Org. Geochem.* **1990**, *16*, 511−519.
(83) Fazeelat, T.; Alexander, R.; Kagi, R. I. Extended 8,14-secohopanes in some seep oils from Pakistan. *Org. Geochem.* **1994**, *21*, 257−264.
(84) Hussler, G.; Connan, J.; Albrecht, P. Novel families of tetra- and hexacyclic aromatic hopanoids predominant in carbonate rocks and crude oils. *Org. Geochem.* **1984a**, *6*, 39−49.
(85) Hussler, G.; Albrecht, P.; Ourisson, G.; Cesario, M.; Guilhem, J.; Pascard, C. Benzohopanes, a novel family of hexacyclic geomarkers in sediments and petroleums. *Tetrahedron Lett.* **1984b**, *25*, 1179−1182.
(86) Villar, H. J.; Püttmann, W.; Wolf, M. Organic geochemistry and petrography of Tertiary coals and carbonaceous shales from Argentina. *Org. Geochem.* **1988**, *13*, 1011−1021.
(87) Killops, S. D. Novel aromatic hydrocarbons of probable bacterial origin in a Jurassic lacustrine sequence. *Org. Geochem.* **1991**, *17*, 25−36.
(88) Killops, S. D.; Massoud, M. S.; Scott, A. C. Biomarker characterisation of an oil and its possible source rock from offshore Korea Bay Basin. *Appl. Geochem.* **1991**, *6*, 143−157.
(89) Rohmer, M.; Bouvier-Navé, P.; Ourisson, G. Distribution of hopanoid triterpenes in prokaryotes. *J. Gen. Microbiol.* **1984**, *130*, 1137−1150.
(90) Ourisson, G.; Albrecht, P.; Rohmer, M. The Microbial Origin of Fossil Fuels. *Sci. Am.* **1984**, *251*, 44−51.
(91) Xiao, H.; Li, M.; Wang, W.; You, B.; Liu, X.; Yang, Z.; Liu, J.; Chen, Q.; Uwiringiyimana, M. Identification, distribution and geochemical significance of four rearranged hopane series in crude oil. *Org. Geochem.* **2019**, *138*, 103929.
(92) Härtner, T.; Straub, K. L.; Kannenberg, E. Occurrence of hopanoid lipids in anaerobic Geobacter species. *FEMS Microbiol. Lett.* **2005**, *243*, 59−64.
(93) Hayes, J. M. Factors controlling 13C contents of sedimentary organic compounds: Principles and evidence. *Mar. Geol.* **1993**, *113*, 111−125.
(94) Sakata, S.; Hayes, J. M.; McTaggart, A. R.; Evans, R. A.; Leckrone, K. J.; Togasaki, R. K. Carbon isotopic fractionation associated with lipid biosynthesis by a cyanobacterium: Relevance for interpretation of biomarker records. *Geochim. Cosmochim. Acta* **1997**, *61*, 5379−5389.
(95) Wang, G.; Wang, T.-G.; Simoneit, B. R. T.; Zhang, L. Investigation of hydrocarbon biodegradation from a downhole profile in Bohai Bay Basin: implications for the origin of 25-norhopanes. *Org. Geochem.* **2013**, *55*, 72−84.
(96) Peters, K. E.; Moldowan, J. M.; McCaffrey, M. A.; Fago, F. J. Selective biodegradation of extended hopanes to 25-norhopanes in petroleum reservoirs. Insights from molecular mechanics. *Org. Geochem.* **1996**, *24*, 765−783.
(97) Bost, F. D.; Frontera-Suau, R.; McDonald, T. J.; Peters, K. E.; Morris, P. J. Aerobic biodegradation of hopanes and norhopanes in Venezuelan crude oils. *Org. Geochem.* **2001**, *32*, 105−114.
(98) Frontera-Suau, R.; Bost, F. D.; Mcdonald, T. J.; Morris, P. J. Aerobic biodegradation of hopanes and other biomarkers by crude oil-degrading enrichment cultures. *Environ. Sci. Technol.* **2002**, *36*, 4585−4592.
(99) Jiménez, N.; Morris, B. E. L.; Cai, M.; Gründger, F.; Yao, J.; Richnow, H. H.; Krüger, M. Evidence for in situ methanogenic oil degradation in the Dagang oil field. *Org. Geochem.* **2012**, *52*, 44−54.
(100) Ding, W.; Hou, D.; Jiang, L.; Jiang, Y.; Wu, P. High abundance of carotanes in the brackish-saline lacustrine sediments: A possible cyanobacteria source? *Int. J. Coal Geol.* **2020**, *219*, 103373.
(101) Wei, L. S. L. W. H. Ring D aromatized 8,14-secohopanes in crude oils and source rocksits geochemical significance. *Acta Sedimentol. Sin.* **1988**, *3*, 41−49.
(102) Wei, H.; Isaksen, G. H. A new maturity parameter based on monoaromatic hopanoids. *Org. Geochem.* **1989**, *16*, 1007−1013.
(103) Wenger, L. M.; Isaksen, G. H. Control of hydrocarbon seepage intensity on level of biodegradation in sea bottom sediments. *Org. Geochem.* **2002**, *33*, 1277−1292.
(104) Köster, J.; Rospondek, M.; Schouten, S.; Kotarba, M.; Zubrzycki, A.; Sinninghe Damsté, J. S. Biomarker geochemistry of a foreland basin: the Oligocene Menilite Formation in the Flysch Carpathians of southeast Poland. *Org. Geochem.* **1998**, *29*, 649−669.
(105) Aichner, B.; Wilkes, H.; Herzschuh, U.; Mischke, S.; Zhang, C. Biomarker and compound-specific δ13C evidence for changing environmental conditions and carbon limitation at Lake Koucha, eastern Tibetan Plateau. *J. Paleolimnol.* **2010**, *43*, 873−899.
(106) Peters, K. E.; Walters, C. C.; Moldowan, J. M. *The Biomarker Guide: Biomarkers and Isotopes in Petroleum Exploration and Earth History*, 2, ed.; Cambridge University Press: Cambridge, 2005.
(107) Sinninghe Damsté, J. S.; Irene, W.; Rijpstra, C.; de Leeuw, J. W.; Schenck, P. A. Origin of organic sulphur compounds and sulphur-containing high molecular weight substances in sediments and immature crude oils. *Org. Geochem.* **1988**, *13*, 593−606.
(108) Sinninghe Damsté, J. S.; Rijpstra, W. I. C.; de Leeuw, J. W.; Schenck, P. A. The occurrence and identification of series of organic sulphur compounds in oils and sediment extracts: II. Their presence in samples from hypersaline and non-hypersaline palaeoenvironments and possible application as source, palaeoenvironmental and maturity indicators. *Geochim. Cosmochim. Acta* **1989**, *53*, 1323−1341.
(109) Sinninghe Damsté, J. S.; Eglinton, T. I.; de Leeuw, J. W.; Schenck, P. A. Organic sulphur in macromolecular sedimentary organic matter: I. Structure and origin of sulphur-containing moieties in kerogen, asphaltenes and coal as revealed by flash pyrolysis. *Geochim. Cosmochim. Acta* **1989**, *53*, 873−889.
(110) Werne, J. P.; Lyons, T. W.; Hollander, D. J.; Formolo, M. J.; Sinninghe Damsté, J. S. Reduced sulfur in euxinic sediments of the


https://doi.org/10.1021/acsomega.1c02762
*ACS Omega* 2021, 6, 30298−30314

Cariaco Basin: sulfur isotope constraints on organic sulfur formation. *Chem. Geol.* **2003**, *195*, 159−179.
(111) Sinninghe Damste, J. S.; Ten Haven, H. L.; de Leeuw, J. W.; Schenck, P. A. Organic geochemical studies of a Messinian evaporitic basin, northern Apennines (Italy)-II*. Isoprenoid and n -alkyl thiophenes and thiolanes. *Org. Geochem.* **1986**, *10*, 791−805.
(112) Machel, H. G.; Krouse, H. R.; Sassen, R. Products and distinguishing criteria of bacterial and thermochemical sulfate reduction. *Appl. Geochem.* **1995**, *10*, 373−389.
(113) Farrimond, P.; Head, I. M.; Innes, H. E. Environmental influence on the biohopanoid composition of recent sediments. *Geochim. Cosmochim. Acta* **2000**, *64*, 2985−2992.
(114) Talbot, H. M.; Summons, R.; Jahnke, L.; Farrimond, P. Characteristic fragmentation of bacteriohopanepolyols during atmospheric pressure chemical ionisation liquid chromatography/ion trap mass spectrometry. *Rapid Commun. Mass Spectrom.* **2003**, *17*, 2788−2796.
(115) Haven, H. L. T.; Leeuw, J. W. D.; Peakman, T. M.; Maxwell, J. R. Anomalies in steroid and hopanoid maturity indices. *Geochim. Cosmochim. Acta* **1986**, *50*, 853−855.
(116) Rosa-Putra, S.; Nalin, R.; Domenach, A.-M.; Rohmer, M. Novel hopanoids from Frankia spp. and related soil bacteria. Squalene cyclization and significance of geological biomarkers revisited. *Eur. J. Biochem.* **2001**, *268*, 4300−4306.
(117) Jiang, L.; George, S. C. Biomarker signatures of Upper Cretaceous Latrobe Group petroleum source rocks, Gippsland Basin, Australia: Distribution and geological significance of aromatic hydrocarbons. *Org. Geochem.* **2019**, *138*, 103905.
(118) Nytoft, H. P.; Vuković, N. S.; Kildahl-Andersen, G.; Rise, F.; Životić, D. R.; Stojanović, K. A. Identification of a Novel Series of Benzohopanes and Their Geochemical Significance. *Energy Fuels* **2016**, *30*, 5563−5575.
(119) Wang, T. G.; Simoneit, B. R. T.; Philp, R. P.; Yu, C. P. Extended 8$\beta$(H)-Drimane and 8,14-Secohopane Series in a Chinese Boghead Coal. *Energy Fuels* **1990**, *4*, 177−183.
(120) Jiang, Z.; Fowler, M. G.; Lewis, C. A.; Philp, R. P. Polycyclic alkanes in a biodegraded oil from the Kelamayi oilfield, northwestern China. *Org. Geochem.* **1990**, *15*, 35−46.
(121) Schaeffer, P.; Trendel, J.-M.; Albrecht, P. An unusual aromatization process of higher plant triterpenes in sediments. *Org. Geochem.* **1995**, *23*, 273−275.
(122) Elvert, M.; Niemann, H. Occurrence of unusual steroids and hopanoids derived from aerobic methanotrophs at an active marine mud volcano. *Org. Geochem.* **2008**, *39*, 167−177.
(123) Cross, M. M.; Manning, D. A. C.; Bottrell, S. H.; Worden, R. H. Thermochemical sulphate re- duction (Tsr): experimental determination of reaction kinetics and implications of the observed reaction rates for petroleum reservoirs. *Org. Geochem.* **2004**, *35*, 393−404.
(124) Li, S.; Shi, Q.; Pang, X.; Zhang, B.; Zhang, H. Origin of the unusually high dibenzothiophene oils in tazhong-4 oilfield of tarim basin and its implication in deep petroleum exploration. *Org. Geochem.* **2012**, *48*, 56−80.
(125) Sinninghe Damsté, J. S.; Schouten, S.; van Duin, A. C. T. Isorenieratene derivatives in sediments: possible controls on their distribution. *Geochim. Cosmochim. Acta* **2001**, *65*, 1557−1571.
(126) Koopmans, M. P.; Schouten, S.; Kohnen, M. E. L.; Sinninghe Damsté, J. S. Restricted utility of aryl isoprenoids as indicators for photic zone anoxia. *Geochim. Cosmochim. Acta* **1996**, *60*, 4873−4876.
(127) Xu, H.; George, S. C.; Hou, D. The occurrence of isorenieratane and 24-n-propylcholestanes in Paleogene lacustrine source rocks from the Dongying Depression, Bohai Bay Basin: Implications for bacterial sulfate reduction, photic zone euxinia and seawater incursions. *Org. Geochem.* **2019**, *127*, 59−80.
(128) Grice, K.; Schouten, S.; Peters, K. E.; Sinninghe Damsté, J. S. Molecular isotopic characterisation of hydrocarbon biomarkers in Palaeocene-Eocene evaporitic, lacustrine source rocks from the Jianghan Basin, China. *Org. Geochem.* **1998**, *29*, 1745−1764.
(129) Schwark, L.; Frimmel, A. Chemostratigraphy of the Posidonia black shale, SW- Germany: II. Assessment of extent and persistence of photic-zone anoxia using aryl isoprenoid distributions. *Chem. Geol.* **2004**, *206*, 231−248.
(130) Madigan, M. T.; Martinko, J. M.; Dunlap, P. V.; Clark, D. P. *Brock Biology of Microorganisms*; Pearson Benjamin Cummings: San Francisco, 2009.
(131) Sousa Júnior, G. R.; Santos, A. L. S.; de Lima, S. G.; Lopes, J. A. D.; Reis, F. A. M.; Santos Neto, E. V.; Chang, H. K.; Chang, H. K. Evidence for euphotic zone anoxia during the deposition of Aptian source rocks based on aryl isoprenoids in petroleum, Sergipe−Alagoas Basin, northeastern Brazil. *Org. Geochem.* **2013**, *63*, 94−104.
(132) Didyk, B. M.; Simoneit, B. R. T.; Brassell, S. C.; Eglinton, G. Organic geochemical indicators of palaeoenvironmental conditions of sedimentation. *Nature* **1978**, *272*, 216−222.
(133) Machel, H. G. Bacterial and thermochemical sulfate reduction in diagenetic settings-old and new insights. *Sediment. Geol.* **2001**, *140*, 143−175.
(134) Burhan, R. Y. P.; Trendel, J. M.; Adam, P.; Wehrung, P.; Albrecht, P.; Nissenbaum, A. Fossil bacterial ecosystem at methane seeps: origin of organic matter from Be'eri sulfur deposit. *Israel Geochim. Cosmochim. Acta* **2002**, *66*, 4085−4101.
(135) Xie, X.; Borjigin, T.; Zhang, Q.; Zhang, Z.; Qin, J.; Bian, L.; Volkman, J. K. Intact microbial fossils in the Permian Lucaogou Formation oil shale, Junggar Basin, NW China. *Int. J. Coal Geol.* **2015**, *146*, 166−178.
(136) Garcia, J.-L.; Patel, B. K. C.; Ollivier, B. Taxonomic, Phylogenetic, and Ecological Diversity of Methanogenic Archaea. *Anaerobe* **2000**, *6*, 205−226.
(137) Kankaala, P.; Huotari, J.; Peltomaa, E.; Saloranta, T.; Ojala, A. Methanotrophic activity in relation to methane efflux and total heterotrophic bacterial production in a stratified, humic, boreal lake. *Limnol. Oceanogr.* **2006**, *51*, 1195−1204.


https://doi.org/10.1021/acsomega.1c02762
*ACS Omega* 2021, 6, 30298−30314